PROTEIN ADSORPTION
on
AMINO ACID CONJUGATED SELF ASSEMBLED MOLECULES

by

SEZİN EREN

B.S., Biomedical Engineering, Yeditepe University, 2012

Submitted to the Institute of Biomedical Engineering
in partial fulfillment of the requirements
for the degree of
Master of Science
in
Biomedical Engineering

Boğaziçi University
2015

ACKNOWLEDGMENTS

I would like to thank my advisor, Assist. Prof. Dr. Bora Garipcan, for his guidance and advices. I thank Assoc. Dr. Deniz Hür, Assoc. and Dr. Lokman Uzun for their help.

I would also like to thank to my committee members Assist. Prof. Dr. Duygu Ege. and Assist. Prof. Dr. Ayşe Ak for their encouragement and insightful comments.

In addition, I would like to give special thanks to my family for the support they provided me through my entire life. Words cannot express how grateful I am to my mother, my father and for all of the sacrifices that they've made on my behalf.

Furthermore, I would like to thank my friends, Özgen Öztürk, Bengü Aktaş, Eren Demirbüken, Agah Karakuzu, Samet Kocatürk, Murat Can Mutlu, Elif Dönmez, and all my laboratory colleagues for their support, understanding and motivation.

This thesis was supported by TÜBİTAK under Project No. 112T564 and by Bogaziçi University Research Fund with Grant Number: 6701 and 7567.

ABSTRACT

PROTEIN ADSORPTION on AMINO ACID CONJUGATED SELF ASSEMBLED MOLECULES

In this thesis, novel amino acid (conjugated histidine, leucine, serine, tryptophan) conjugated self-assembled molecules (SAMs) were synthesized and used to modify model metallic [Gold, (Au)] and inorganic [Silicon Oxide, (SiO_2)] surfaces to investigate protein adsorption. In the first step, Au and SiO_2 surfaces were cleaned and modification of surfaces were carried out with 3-mercaptopropanoyl and 3 - (trimethoxysilyl)propane functional groups conjugated amino acids (for Au; histidine, leucine, serine, tryptophan, for SiO_2; histidine and leucine), respectively. Syntheses of amino acid conjugated SAMs were characterized with ^{1}H-Nuclear Magnetic Resonance (^{1}H-NMR) Spectroscopy. Au and SiO_2 surfaces modified with amino acid conjugated SAMs were characterized water contact angle measurements. We aimed to manipulate and change the adsorption of the proteins (Albumin, Fibrinogen and Immunoglobulin G) on these surfaces using amino acid conjugated SAMs. Protein adsorption was investigated in-situ by using Quartz Crystal Microbalance (QCM) biosensors. According to results, target proteins have shown different affinity to the amino acid conjugated Au and SiO_2 coated crystals depending the type of the amino acids and concentration. For instance, according to comparison of Histidine modified SiO_2 and Au surfaces, properties of surfaces have shown a clear difference and effect on protein adsorption. In addition, according to comparison of Leucine modified SiO_2 and Au surfaces, properties of surfaces have shown a clear effect on protein adsorption as having the same surface chemistry. Consequently, it has been observed that these controlled chemistry on the surfaces of materials have a great potential to manipulate protein adsorption for biomedical applications.

Keywords: Self-Assembled Monolayers, Amino acids, Surface Modification, Protein Adsorption, Quartz Crystal Microbalance (QCM) Biosensors.

ÖZET

AMİNO ASİT KONJUGE KENDİLİĞİNDEN DÜZENLENEN MOLEKÜLLER İLE PROTEİN ADSORPSİYONUNUN ARAŞTIRILMASI

Bu tez çalışmasında, metalik [Altın, (Au)]ve inorganik [Silisyum Oksit, (SiO_2)] yüzeyler, yeni sentezlenen amino asitler ile konjuge kendiliğinden düzenlenmiş moleküller (KDM) (konjuge amino asit histidin, lözin, serine ve triptofan) ile modifiye edilerek, protein adsorpsiyonları incelenmiştir. İlk aşamada yüzeylerin temizlenmesi ve yüzeylerin 3-merkaptopropanol and 3-(trimetoksilil)propan ile fonksiyonel grupları ile konjuge amino asitler ile yüzeylerin modifiyesi gerçekleştirilmiştir (Au için histidin, lözin, serin, triptofan, SO_2 için histidin and lözin). Daha sonra sentezlenen amino asit konjuge KDMler ^{1}H-Nükleer Manyetik Rezonans (^{1}H-NMR) Spektroskopi yöntemi ile karakterize edilmiştir. Amino asit konjuge KDMler ile modifiye edilen yüzeyler temas ölçüm açısı ölçme yöntemi ile karakterize edilmiştir. Bu çalışmada protein adsorpsiyonunun (Albumin, Fibrinojen and Immünoglobulin G), amino asit konjuge yüzeyler kullanılarak değiştirilmesi manipule edilmesidir. Protein adsorpsiyonu Kuartz Kristal Mikroterazi biyosensör kullanılarak yerinde incelenmiştir. Sonuçlara göre kullanılan proteinler aimno asit konjuge KDMerle modifiye yüzeylere amino asit çeşidi ve konsantrasyona bağlı olarak değişik afinite özellikleri göstermiştir. Örneğin, Histidin modifiye Au ve SiO_2 yüzeylerde protein adsorpsiyonu açık bir şekilde farklılık göstermiştir. Ek olarak, Lözin modifiye Au ve SiO_2 yüzeylerde protein adsorpsiyonunda aynı yüzey kimyasına bağlı olarak yakın sonuçlar elde edilmiştir. Sonuç olarak malzemelerin kontrollü yüzey kimyasının protein adsopsiyon manüplasyonu için biyomedikal uygulamalarda büyük bir potansiyelinin olduğu gözlenmiştir.

Anahtar Sözcükler: Kendiliğinden Düzenlenen Moleküller, Yüzey Modifikasyonu, Protein Adsorpsiyonu, Kuartz Kristal mikroterazi, biyosensör

TABLE OF CONTENTS

LIST OF FIGURES

LIST OF TABLES

LIST OF SYMBOLS

Δ	Delta

LIST OF ABBREVIATIONS

Au	Gold
Si	Silicon
APTES	Tunneling Scanning Microscope
SAM	Self-Assembled Molecule
His-SAM	Histidine conjugated Self-Assembled Molecules
Leu-SAM	Leucine conjugated Self-Assembled Molecules
Ser-SAM	Serine conjugated Self-Assembled Molecules
Trp-SAM	Tryptophan conjugated Self-Assembled Molecules
QCM	Quartz Crystal Microbalance
ECM	Extra Cellular Matrix
NMR	Nuclear Magnetic Resonance
PVD	Physical Vapor Deposition
CVD	Chemical Vapor Deposition
PECVD	Plasma Enhanced Chemical Vapor Deposition
SEM	Scanning Electron Microscopy
AFM	Atomic Force Microscopy
TEM	Tunneling Electron Microscope
TSM	Tunneling Scanning Microscope
FTIR	Fourier Transform Infrared Spectroscopy
IgG	Immunoglubulin G
TLC	Thin Layer Chromatography
RT	Room Temperature
Hz	Hertz

1. INTRODUCTION

1.1 Motivation

Biomaterials have tremendous role in the achievement of medical devices and medicine, especially designing synthetic replacements for biological tissues, designing materials for specific medical applications, and biomaterials for new applications such as diagnostics [1]. A biomaterial is any build made specifically to interact with biological systems; therefore, it must have properties (e.g. stiffness, chemical composition, biological signals) compatible with the tissue it will interact with in order to obtain the desired effect [2]. The major concern is insufficient or improper interactions between the synthetic materials and living systems. Modification of the surface of the biomaterials is the common strategy to solve this problem. To enhance the biocompatibility, surfaces are modified with functional molecules such as amino acids, isolating single molecules, pairs of molecules, one-dimensional lines of molecules, or larger groups of molecules [3], [4].

Some organic molecules have been called as self-assemble biomaterials, including synthetic polymers; materials based on naturally occurring components such as biopolymers and, more recently, molecularly designed materials based on biological structural units such as amino acids, peptides and proteins. Self-assemble is the novel approach to form from molecular components into supramolecular structures. The self-assemble structures are association of an ensemble of molecules into one or more supramolecular structures, driven by multiple noncovalent interactions to modify surfaces [2]. A self-assembled monolayer (SAM) consists of a single layer of individual molecular chains that spontaneously chemisorb onto a surface which provides functionalization of the surface to effect specific protein adsorption [5].

Biocompatibility of the biomaterials is the important scientific issue that is investigated as biomaterial-protein interactions and biomaterial-cell interactions. As

the matter of the fact, protein adsorption is occurred first, then cell adhesion and growth are observed, when biomaterials are implanted in vivo or tested in vitro [6]. Surface chemistry, surface topography and mechanical properties of the biomaterials are very important factors that affect the protein adsorption. The success of implant application is determined in very early stages by reactions of the primary adsorbing species of the body fluids. Due to that reason, protein adsorption has vital role during implantation. In many cases, protein adsorption is necessary and required, for instance manipulating cell adhesion. To sum up, protein adsorption is a dynamic process that includes binding, rearrangement, and detachment. Ideal biomaterial should be able to support these interactions, therefore surface modification has significance role to evolve with inclusion of targeted adsorbents [7]. In this situation, self-assembled monolayers can be very helpful to modify the surface of biomaterials. For instance, self-assembled monolayers can be used to immobilize enzyme on surface of biomaterials. As a result, self-assembled layers can be used for cell adhesion and protein interaction studies [8].

Quartz Crystal Microbalance (QCM) is the one of the surface characterization techniques that can be used for protein adsorption investigation. QCM has ability to recognize behavior biochemical molecules through changes of resonance frequencies of the quartz plate. Quartz plate can adsorb target molecules, resulting in increase of the mass and in the decrease of resonance frequencies [9].

Base on this information, protein adsorption may be affected by newly synthesized different type of self-assembled monolayers, which are [Histidine-Self Assembled Molecule (His-SAM), and Leucine-Self Assembled Molecule (Leu-SAM) for SiO_2 surfaces and Histidine-Self Assembled Molecule (His-SAM), and Leucine-Self Assembled Molecule (Leu-SAM) Serine-Self Assembled Molecule (Ser-SAM) and Tryptophan-Self Assembled Molecule (Trp-SAM)] for Au surfaces. The characterizations of these samples can be analyzed with nuclear magnetic resonance (NMR), contact angle measurements and QCM. By using QCM, the investigation of surface modification and protein adsorption also can be performed.

1.2 Objectives

In this study, SiO_2 and Au model surfaces were used as substrates. SiO_2 and Au surface specific molecules were synthesized which are conjugated with histidine, leucine, serine and tryptophan due to their biological importance, building blocks of proteins and part of extracellular matrix to investigate protein adsorption. The main objectives of this study are:

- To synthesize new SAMs,
- To investigate protein adsorption of amino acid conjugated self-assembled molecules modified SiO_2 and Au substrates,
- To evaluate biocompatibility of SAM modified SiO_2 and Au surfaces.

1.3 Outline

This thesis is presented as follows: In chapter 2, background information about self-assembled monolayers, surface modification, and protein adsorption and QCM biosensors is given. In chapter 3, the experimental procedures are explained. In chapter 4, the results are presented. In chapter 5, the discussion of the results is given.

2. BACKGROUND

Surface and biological environment interactions are very important in the fields of biology, biotechnology and medicine. Hence the surface of a biomaterial becomes very significance for existing applications such as, studies in molecular and cell biology, tissue engineering, and implant devices [10]. Engineering of biological activity into synthetic materials increases their potential uses and improves their performance in more traditional applications. Besides, functionality and complexity of biological systems caused scientists inspiration to design like natural materials. Designing new biomaterials is inspired from structure-function analysis on various length scales of the extracellular materials that cells use to organize themselves into tissues. Biological interactions with surfaces were regulated by nonspecific adsorption of serum protein layers. The adsorption of extracellular matrix (ECM) proteins is an important research area that how surface chemistry and topography affect. However, engineering of the surface of materials is very difficult to adsorb accurate mixture and arrangement of ECM proteins [11]. Due to that reason, biomaterial design and surface modification gain important role in this area to improve biomaterials and tissue interactions.

2.1 Surface Modification Techniques

During biomaterials-tissue interactions, biological responses are controlled by many factors, but scientists commonly accept that surface properties of a biomaterial adjust the biological response. Interactions between cell and proteins and host response are moderated by surface properties such as chemistry, topography, surface free energy, elasticity, and charge [12]. Hence, surface modification has significant role, because selected surface properties such as tocompatibility and antimicrobial characteristics can be enhanced while the bulk biomaterials features such as mechanical strength, robustness, and inertness can be preserved [13], [14].

There are a lot of surface modification techniques that are used:

- Thermal Surface modifications provide a wide range of functions to modify the properties of the components spraying [14], [15],
- Plasma spraying [14], [16],
- Physical vapor deposition (PVD) [14], [17],
- Chemical vapor deposition (CVD) [14], [18],
- Plasma enhanced chemical vapor deposition (PECVD) [14], [19],
- Layer by layer assembly [14], [20],
- Sol-gel [21], [22],
- Photolithography [23],
- Silanization and Langmuir-Blodgett deposition [24],
- Immobilization of biomolecules [24], [25],
- Spin coating [26], [27],
- Self-assembled monolayer [25], [28], [29] etc.

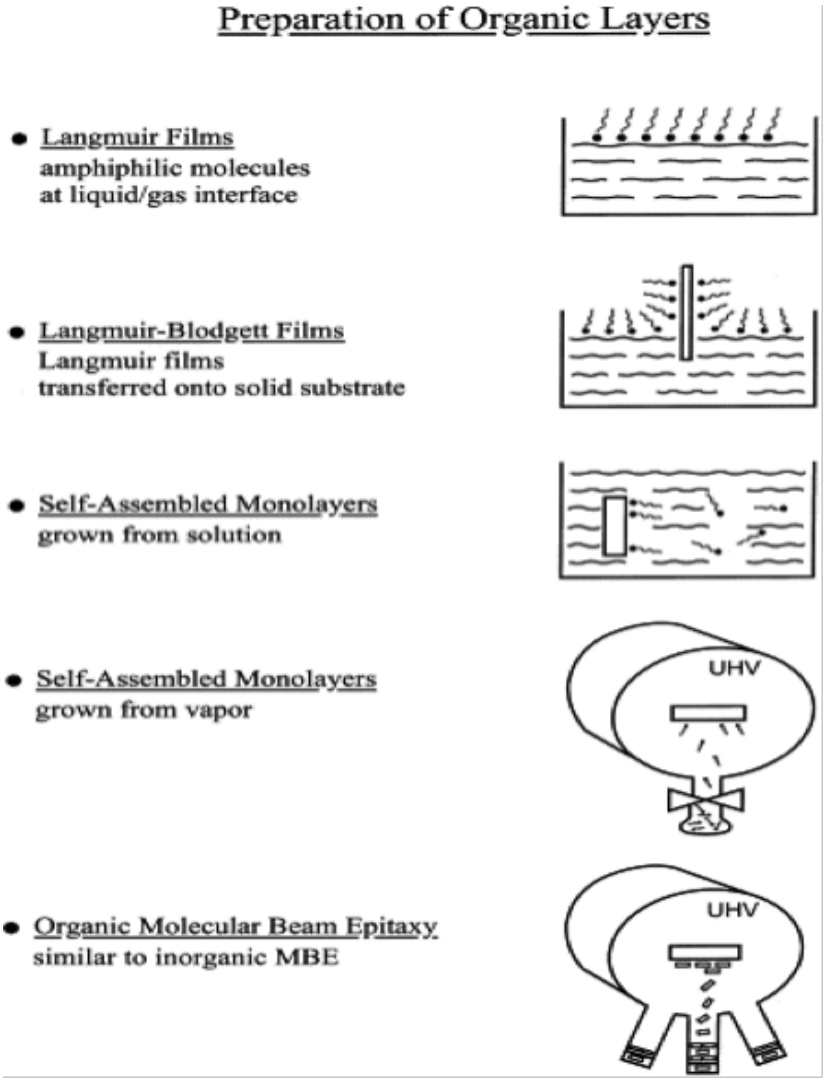

Figure 2.1 Some examples of preparation techniques for organic layers [24].

2.1.1 Self Assembled Monolayers

Self-assembled monolayers are thin organic layers that are formed on the surface in orderly manner. In general, they are long alkyl chain supramolecules, which have special affinity to particular surfaces, and they are attached by chemisorption [22].

The essential of SAMs are the head group or anchoring group, which attaches the molecules to the substrate. The end group defines the state of functionalization of the new outer surface following modification. Functional group or generally called alkyl chain provides an additional driving force for the adsorption reaction via van der Waals interactions and create certain degree of order in the system. In general,

head groups include methyl ($-CH_3$), trifluorocarbon ($-CF_3$), carboxyl (–COOH), amino ($-NH_2$), and biotin. Functional groups (alkyl chains) generally consist of hydrocarbon chains [30].

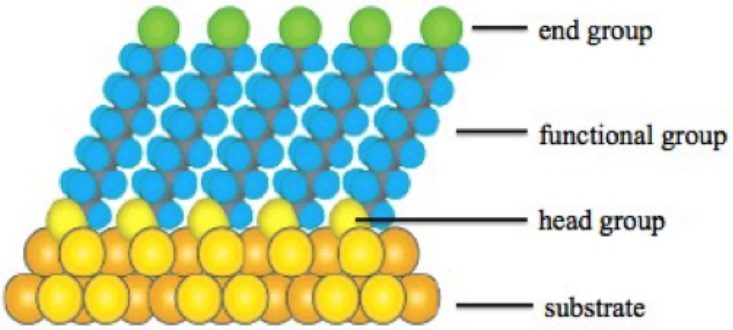

Figure 2.2 Structure of self-assembled monolayer.

Table 2.1
Combinations of Head groups and Substrates Used in Forming SAMs on Metals, Oxides, and Semiconductors [31] .

Self-Assemled Monolayers		
Surface	**Ligand**	**Bond**
Au	RSH, ArSH (thiol)	RS-Au
Au	RSSR (disulphide)	RS-Au
Au	RSR (sulphite)	RS-Au
SiO_2	RSiCl3, RSiOR3	Siloxane
Glass	[RCOO]2	R-Si
Si	RCH=CH2	R-CH_2CH_2-Si
Si	RSH	RS-GaAs
GaAs	RSH, ArSH	RS-Ag
Ag	RSH, ArSH	RS-Cu
Cu	RCOOH	RCO_2-.....MOn
Metal oxides	RCONHOH	RCONHOH.....MOn
Metal Oxides	RSH, ArSH	RCONHO-.....MOn
Pt	RNC	RS-Pt
Pt		RNC-Pt
Ti	Phosphonic Acid	Ti-P

SAMs are preferable to study for some reasons:

- Easy to prepare,
- The adjustability of surface properties via modification of molecular structure and functions,
- The use of SAMs as building blocks in more complex structures to colligate additional layer to the surface,
- The possibility of lateral structuring in the nanometer order [25].

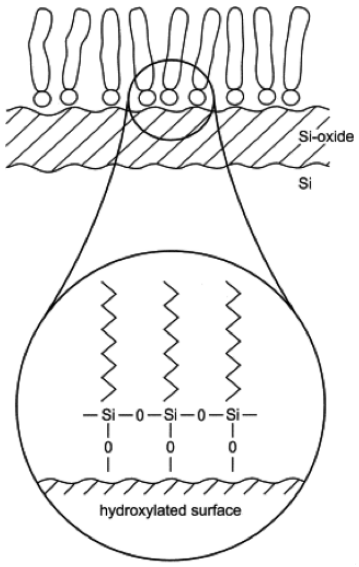

Figure 2.3 Schematic of monolayer of n-alkyltrichlorosilane $CH_3-(CH_2)_{n-1}-SiCl_3$ on hydroxylated surface like silicon oxide [25].

In this study, amino acids such as histidine, leucine, serine, and tryptophan were used in form of conjugated self-assembled molecules due to their biological duties. For instance, leucine is an essential amino acid that helps regulation of protein metabolism and maintenance of muscle proteins [32]. Histidine is also an essential amino acid, which is precursor of histamine and a neurotransmitter [33] In that manner, tryptophan is an amino acid, and shows antimicrobial effect [34]. Serine is non-essential amino acid that is important in various biosynthetic pathways. In addition, it is the pioneer to a number of amino acids like glycine and cysteine. Besides, it helps an enzyme catalyze its reaction which is hydrolysis of peptide bonds in polypeptides and proteins, that is a major function in the digestive process [35].

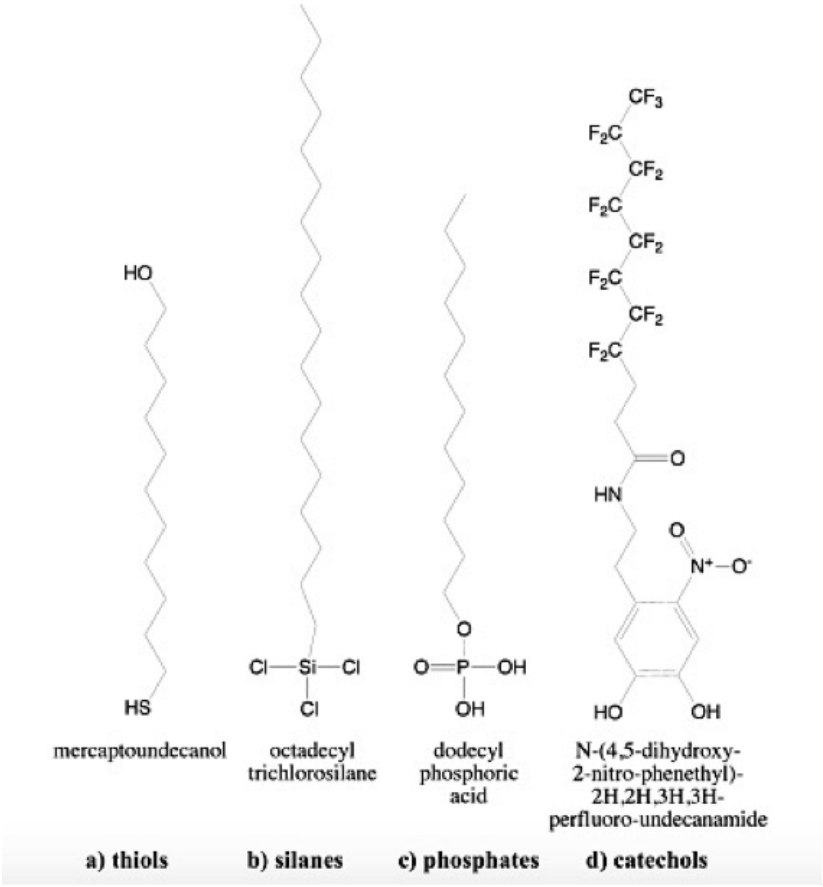

Figure 2.4 Examples of molecules that have been used to produce self-assembly monolayers on various surfaces [31].

2.2 Protein Adsorption

Proteins are the one of the important building blocks of human body that has significant roles. For instance, establishment and maintenance of structure that means structural proteins are responsible for the shape and stability of cells and tissues. The other issue is transportation of ions and other biological metabolites. Some proteins are responsible for protection of the body from pathogens and foreign substances in the immune system. Hormones are also made from proteins that provide biochemical signal as hormone receptors to control and regulation of the body homeostasis. Some enzymes are made from proteins to catalysis. In addition, proteins have movement and storage duty in the body [35]. In that manner, biological fluids, especially blood includes proteins in addition to other constituents. Proteins are major constituents of the blood that are albumin, immunoglobulins and fibrinogen as proteins. Albumin is a globular protein and the most abundant component of many biological fluids serving the transport of various metabolites and the regulation of the osmotic pressure [36], [37]. Immunoglobulins are also called antibodies that are glycoprotein molecules produced by plasma cells. They have significant role in the immune response with specifically recognizing and binding to particular antigens duties. The various immunoglobulin isotypes differ in their biological features, structure, target specificity and distribution. IgG is the one of the isotypes of the immunoglobulins that is the key player in the humoral immune response [38]. Fibrinogen is one of the main proteins involved in the blood coagulation cascade [39]. In some cases, fibrinogen layers formed at the liquid-solid implant interface, and they have triggered an inflammatory response and have been a part of some of the process that may start to process to acceptance or rejection of the implant [40]. During the interaction between biological fluids and biomaterials, adsorption of these proteins is observed on the surface [41].

Protein adsorption on surfaces is a major issue for the rational design and application of biomaterials. The rate and strengths of the first physical interactions between proteins and surfaces show the final confirmation, stability and activity of such proteins. This issue determines biocompatibility of materials [42].

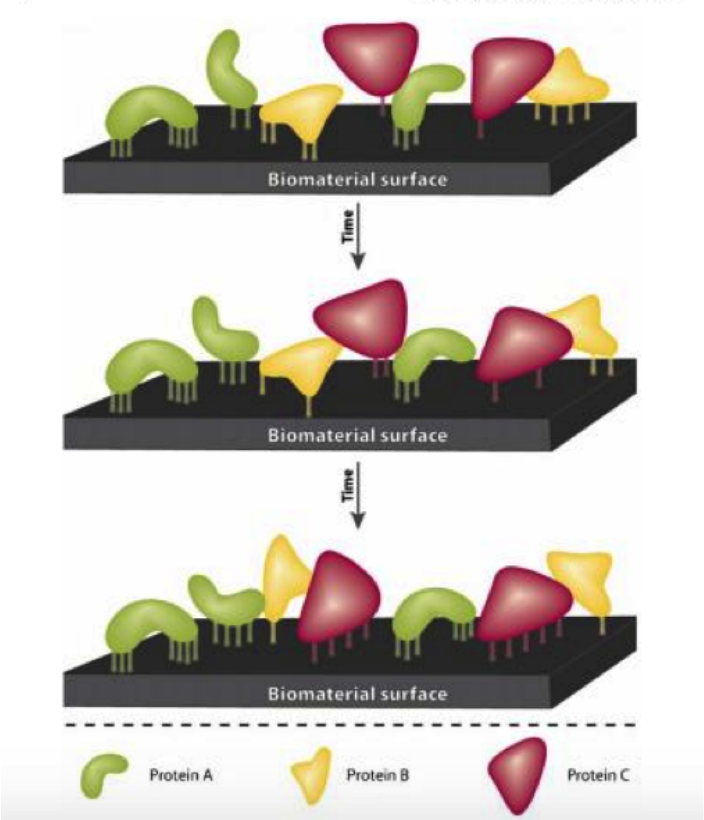

Figure 2.5 Protein adsorption scheme [43].

"Adsorption" is defined as adherence of a molecule to the surface of a solid and should not be confused with the term "absorption". That means the molecule is brought into the solid and cells interact with a dynamic coating proteins. The ability to interact with cells and other biological molecules or activity of proteins dictates the initial cellular and subsequent, host response. Protein adsorption to biomaterials is affected by some factors such as the bulk concentration of the protein solutions, rate of diffusion and, affinity [43].

Proteins are built up from 21 different amino acids linked together by peptide bonds and forming highly organized polymers. Protein function depends on its third dimension (3D) arrangement, which is related its amino acid sequence. Each amino acid has the same fundamental structure, including α carbon (Cα) to which an amino group, carboxyl group and a differing variable side chain (R) are bonded [44].

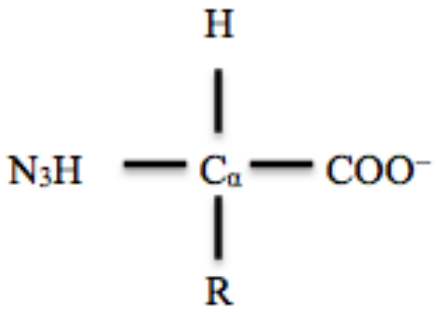

Figure 2.6 Amino acid structure.

Amino acids are usually classified by the properties of the side chain –R group- into four groups. The side chain can provide the amino acid with different properties: acidity, basicity, hydrophilicity, if it is polar, and hydrophobicity if it is non-polar. The chemical structures of the 21 standard amino acids, along with their chemical properties, are catalogued. The secondary structure of proteins refers to folding of the polypeptide chain into periodic structure such as, α-helix and β-sheet, these local structures are stabilized by hydrogen bonds between amide and carboxyl groups. The tertiary structure is referred that the folding segments of the polypeptide chain are arranged in space, as a result the completed three-dimensional folding of a protein. Stabilization of the tertiary structure of a protein may involve interactions between amino acids located distance along the primary sequence. These may include:

- weak interactions such as hydrogen bonds and Van der Waals interactions,
- ionic bonds involving negatively charged and positively charged amino acid side-chain groups,
- disulfide bonds .

The quaternary structure is the non-covalent composition of independent tertiary structures to form a complex [44].

According to this information, structures of proteins and surface properties are

considered important factors for protein adsorption. The factors that affect protein adsorption are summarized in Table 2.2.

Table 2.2
Main surfaces properties that determine protein adsorption [44], [45].

Surface Properties	Protein Properties
Chemistry Surface topography Free energy Charge Acid/Base properties Surface impurities	Bonding number Quaternary, tertiary and secondary structure Overall hydrophobicity Charge Isoelectric point (pI) Specific interacting residues

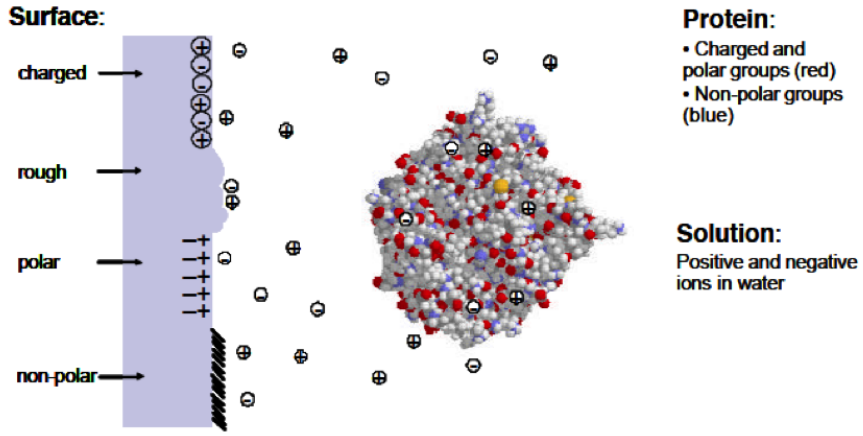

Figure 2.7 Schematic views of a protein and a well-characterized surface [46].

2.3 Quartz Crystal Microbalance Biosensors

In the literature, nanomaterial- protein interface and protein adsorption process are characterized by using a lot of techniques. For instance, atomic force microscopy (AFM), scanning electron microscopy (SEM), transmission electron microscopy (TEM), and tunneling scanning microscopy (TSM) can be used to determine surface features and topography [47]. Every characterization techniques have advantages and disadvantages. AFM can scan 3D images of the surface topography but it could be affected

by a lot of artifacts. With electron microscopy techniques, subatomic levels can be observed, but the sample has to be conductive and it could be harmful at the end of the process. Recently, electron crystallography also is used to determine structure of several proteins to identify them. Also there are other techniques that are used to help to understand protein adsorption investigation such as, capillary electrophoresis, mass spectrometry, particle mass spectrometry and, Fourier-Transform Infrared (FTIR) etc. Among the other techniques, ellipsometry and quartz QCM are also used to investigate protein adsorption [42].

QCM has ability to recognize behavior among extremely small amounts of proteins (mass changes) through changes of resonance frequencies of the quartz crystal plate [42], [48].

Figure 2.8 Cr/Au QCM Crystals.

QCM is used as chemical and biological sensors. It can generate a response to any mass chance on the quartz plate. In general, QCM sensor is used with addition of a sensitive layer on the surface of the crystal. Organic thin layers are preferable coatings techniques due to their capability to reversibly adsorb vapors and liquids. QCM applications show excessive increase in recent years as in field of biochemical analysis. QCM devices are used as biochemical and immunological sensors to investigate and/or monitor of biochemically significant processes, such as self assembled-molecule investigation and protein adsorption investigation [49–54].

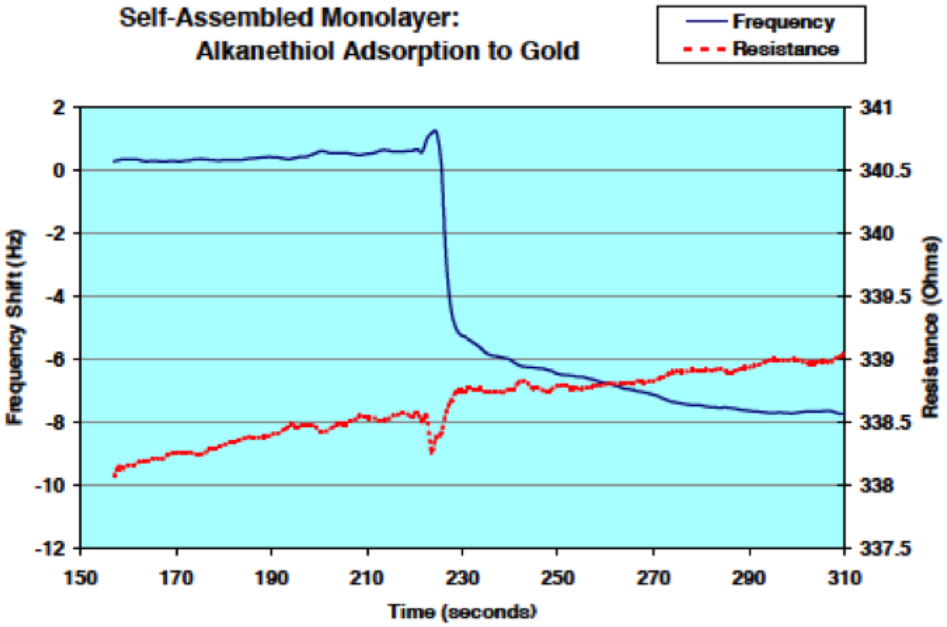

Figure 2.9 Example of self- assembled monolayer adsorption investigation [55].

3. MATERIALS AND METHODS

3.1 Synthesis of Amino Acid Conjugated Self Assembled Molecules

3.1.1 Preparation of 3-(trimethoxysilyl)propan Amino Acids

Novel 2-amino-3-(1H-imidazol-4-yl)-N-(3-(trimethoxysilyl)propyl)propanamide (Histidine-Silane) and 2-amino-4-methyl-N-(3-(trimethoxysilyl)propyl)pentanamide (Leucine-Silane) were prepared using the procedure [56] (Figure 3.1) via N-acylbenzotriazole.

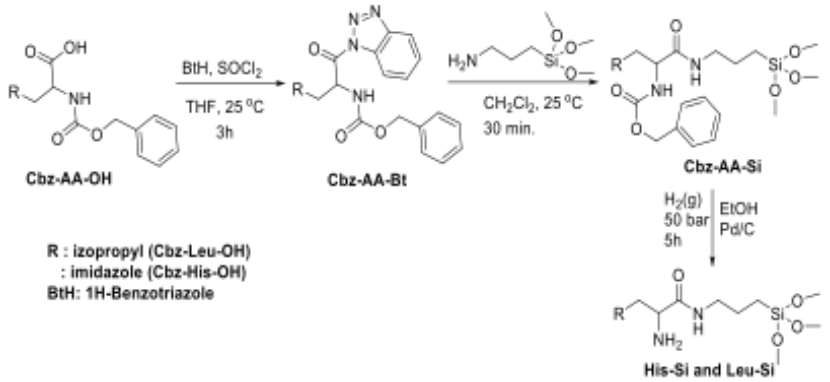

Figure 3.1 Preparation method for 2-amino-3-(1H-imidazol-4-yl)-N-(3(trimethoxysilyl) propyl) propanamide and 2-amino-4-methyl-N- (3- (trimethoxysilyl) propyl)pentanamide.

•Preparation of Cbz-Amino Acid-Bt intermediate (Cbz-AA-Bt)

Benzotriazole (4 eq.) was dissolved in dry THF under N_2 atmosphere at room temperature. Thionyl chloride ($SOCl_2$, 1.2 eq.) was added dropwise to this solution. After 30 min stirring Cbz-Leu-OH or Cbz-His-OH (1 eq.) was added to solution in one portion. Reaction mixture was allowed to stir for additional 3 hours at ambient temperature. After reaction finished the white precipitate was filtered off. The filtrate was concentrated under vacuum to get sticky oil residue. In case of histidine this reaction mixture, which contains Cbz-His-Bt intermediate, was directly used for next reaction without any purification. For Leucine the oily reaction mixture was dissolved in ethylacetate and extracted using 20% aqueous solution of Na_2CO_3 to remove excess benzotriazole. Organic layer was dried over Na_2SO_4 to give benzyl (1-(1H-

benzo[d][1,2,3]triazol-1-yl)-4-methyl-1-oxopentan-2-yl)carbamate (Cbz-Leu-Bt).

• **Preparation of Cbz- [His-Si(OCH_3)]$_3$ and Cbz- [Leu-Si(OCH_3)]$_3$**

3-(trimethoxysilyl)propan-1-amine (1 eq.) was added drop wise to the solution of Cbz-AA-Bt (1 eq.) in CH_2Cl_2 under N_2 atmosphere at RT, reaction was monitored by Thin Layer Chromatography (TLC). After 30 minutes. Reaction mixture was extracted using 10% Na_2CO_3. Organic layer was dried over Na_2SO4 to give Cbz-[His-Si(OCH_3)]$_3$ and Cbz-[Leu-Si(OCH_3)]$_3$.

•**Preparation of [His-Si(OCH_3)]$_3$ and [Leu-Si(OCH_3)]$_3$**

Cbz-AA-Si (1 eq.) was dissolved in methanol (10 mL), Pd/C (3 eq.) was added this mixture and reaction mixture was stirred at stainless still reactor under 50 bar H_2 (g) atmosphere for 5 hours. Catalyst was filtered over Celite. Filtrate was evaporated under vacuum to obtain [His-Si(OCH_3)]$_3$ and [Leu-Si(OCH_3)]$_3$.

3.1.2 Preparation of 3-mercaptopropanoyl Amino Acids

The preparation of 3-mercaptopropanamido amino acids (5) was conducted following (Figure 3.2) multistep synthesis. In summary, the mercapto (-SH) function of 3-mercaptopropionic acid, (1), was protected using acetylation in pyridine. This acetylated propionic acid was activated and converted to N-acylbenzotriazole derivative, 3. Afterwards, intermediate (3) was reacted with different amino acids in presence of NaOH hydroxide in dioxane-water mixture to give mercapto-protected amido amino acids (4). Deprotection using 4N HCl in EtOH, gave novel 3-mercaptopropanoyl amino acids, (5).

• **Synthesis of 3-(acetylthio)propanoic Acid**

Pyridine (3 eq.) was slowly added to the neat mixture of 3-mercaptopropionic

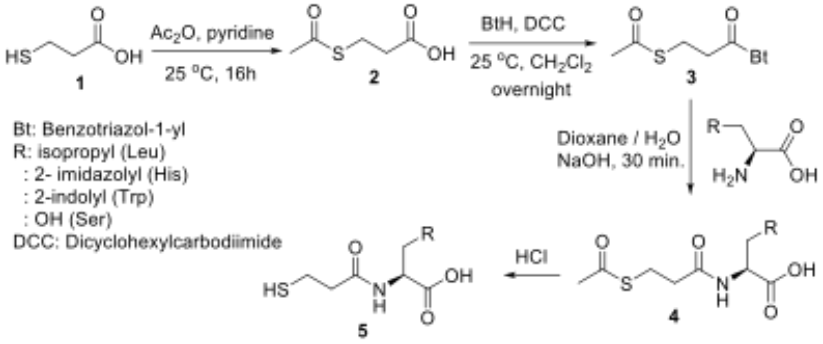

Figure 3.2 General Preparation method for novel 3-mercaptopropanamido amino acids (5).

acid, (1), (1 eq.) and acetic anhydride (3 eq.). The reaction mixture was allowed to stir overnight at RT. Reaction mixture was concentrated under vacuum; obtained crude mixture was dissolved in ether and washed with 0.5 N solution of KHSO4. The organic layers were collected and dried over Na_2SO_4. Solvent was removed under vacuum to give 3-(acetylthio)propionic acid (2).

• Synthesis of S-(3-(1H-benzo[d][1,2,3]triazol-1-yl)-3-oxopropyl) ethanethioate

Benzotriazole (BtH, 1 eq.) was added to the solution of 3-(acetylthio)propanoic acid, 2 (1 eq.) and DCC (1 eq.) in dry dichloromethane in ice bath. The reaction mixture was kept at this temperature for 16 h. The White precipitate was filtered off. Filtrate was extracted with 4N HCl. Organic layer was dried over Na_2SO_4 and concentrated under vacuum to give S-(3-(1H-benzo[d][1,2,3]triazol-1-yl)-3-oxopropyl) ethanethioate (3).

•General synthesis of 3-mercaptopropanoyl Amino Acids (5)

Amino acid (1 eq.) was dissolved in 1N NaOH (1.5 eq.) water solution. S-(3-(1H-benzo[d][1,2,3]triazol-1-yl)-3-oxopropyl) ethanethioate, (3) (1 eq.) was added as an dioxane solution at RT. The reaction mixture was stirred at room temperature 30 min. Dioxane was removed under vacuum. The water solution was extracted with ethyl acetate to remove substituted 1H-benzotriazole. Water layer was acidified using 1N HCl.

Water was removed; crude product was dissolved in EtOH and filtered. 4N HCl was added crude mixture and this mixture was refluxed for 3h to give 3-mercaptopropanoyl amino acids (5).

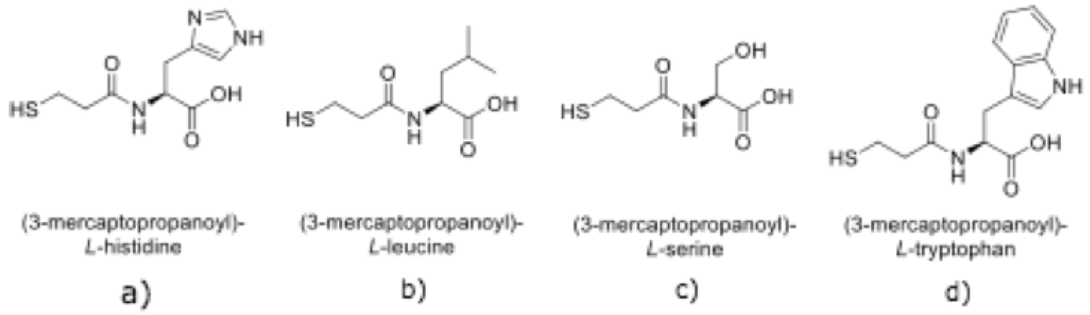

Figure 3.3 Molecular structures of newly synthesis amino acid conjugated self assembled monolayers: a) L-Histidine, b) L-Leucine, c) L-Serine, d) L-Tryptophan.

The characterization of all intermediate byproducts and -trimethoxysilyl)propan amino acids (His-SAM and Leu-SAM) and 3-mercaptopropanoyl amino acids (Histidine-SH; Leucine-SH; Serine-SH and Trytophan-SH) was done by using NMR spectroscopy (Brueker, 500 MHz, Germany) in $CDCl_3$, or DMSO-d6. Tetramethylsilane was used as an internal standard.

3.2 Surface Preparation

3.2.1 Cleaning and Sterilization of QCM Crystals

Ti/Au/Ti/SiO_2 and Cr/Au QCM crystals surfaces were used as substrates to modify and to investigate target protein (Albumin, fibrinogen and immunoglobulin-G) adsorption. The QCM crystals were purchased from Maxtek, USA and Stanford Research Systems, USA (1 inch sensor crystals) are shown in Figure 3.1.

Cleaning process was applied according to QCM manual [57]. The crystals were

Figure 3.4 Cr/Au QCM Crystals.

treated in UV/Ozone (Jelight Company Inc., USA) for 10 minutes. Then, the crystals were immersed into a 1:1:5 solution of H_2O_2 (30%), NH4OH (25%) and deionized water heated to a temperature of about 75°C for 5 minutes [57]. After this process, the crystals were immediately rinsed with distilled water and dry with N_2 gas. Before reuse of the crystals, to remove any remaining surface contaminants, crystals were treated UV/Ozone for 10 minutes immediately before measurement.

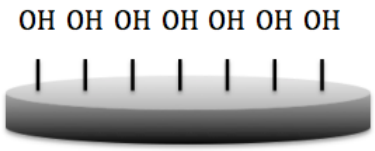

Figure 3.5 Surface activation with UV/Ozone.

3.2.2 Modification of SiO_2 Substrates

After cleaning process, SiO_2 substrates were modified in-situ by amino acid conjugated SAMs (which were His-Silane SAM, Leu-Silane SAM), and (3-Aminopropyl) triethoxysilane (APTES). Modifications of substrates were occurred in situ during measurement. During modification and measurement process, tubing system and peristaltic pump were used to provide influx of amino acid conjugated SAM solutions through the flow cell part of QCM. During measurements, flow rates were kept 0.17mL/min

and constant to prevent signal transient due to pressure and temperature fluctuations. The peristaltic pump was used in low flow rate settings, below 0.2mL/min to assure minimal transient and flow-induced noise in the frequency measurement [57].

Figure 3.6 Flow Cell.

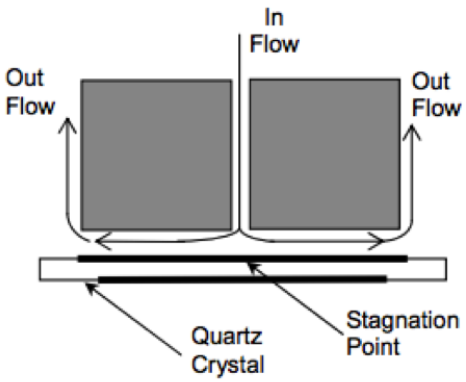

Figure 3.7 Schematic representation of the liquid flow pattern in the Axial Flow Cell [57].

• Modification of SiO_2 Substrates with His-Silane SAM and Leu-Silane SAM

His-Silane SAM and Leu-Silane SAM solutions 10mM each were used to modify in-situ the surfaces of substrates. The modification was observed during experiments via QCM, in terms of frequency change in Hz. Ethanol was used as a solvent of His-Silane SAM and Leu-Silane SAM solutions. 5ml, 10mM His-Silane SAM and Leu-Silane SAM solutions were passed through the flow cell via tubing system by peristaltic pump to modify SiO_2 surfaces.

- **Modification of SiO_2 Substrates with APTES**

10mM APTES solution was used to modify in-situ the surfaces of substrates. The APTES solution was prepared from Sigma Aldrich $\geq$ 98% APTES solution. The modification was observed during experiments via QCM, in terms of frequency change in Hz. Ethanol was used as a solvent of APTES solution. 5ml, 10mM APTES solution was passed through the flow cell via tubing system by peristaltic pump to modify SiO_2 substrates.

3.2.3 Modification of Au Substrates

As SiO_2 substrates, Au QCM crystals were also modified with amino acid conjugated self-assembled monolayers, which were His-SH SAM, Leu-SH SAM, Ser-SH SAM, and Trp-SH SAM. Before modifications, the crystals were immersed in ethanol for 1 hour to remove Au-Oxide islands to prevent hydrophilicity [58].

- **Modification of Au substrates with amino acid conjugated SAMs**

His-SH SAM, Leu-SH SAM, Ser-SH SAM, Trp-SH SAM 10mM each solutions were used to modify in-situ the surfaces of substrates. The modification was observed during experiments via QCM, in terms of frequency change in Hz. Ethanol was used as a solvent of Leu-SH SAM, Ser-SH SAM, Trp-SH SAM solutions. For His-SH SAM solution, dI H_2O water was used as solvent. 5ml, 10mM His-SH SAM, Leu-SH SAM, Ser-SH SAM, Trp-SH SAM solutions were passed through the flow cell via tubing system by peristaltic pump to modify Au QCM surfaces.

3.3 Surface Characterization

3.3.1 Frequency Measurements by QCM

This method is aimed to analyze mass change on metallic and inorganic substrates by monitoring the change in resonance frequency of the quartz crystal (AT cut 5MHz).

Figure 3.8 Quartz Crystal Microbalance Device, Stanford Research Systems, USA.

Sauerbrey recognized the potential usefulness of the Quartz Crystal Microbalance (QCM) technology and demonstrate the tremendously sensitive structure of these piezoelectric devices towards mass changes at the surface of QCM electrodes [59]. The results of his work are incorporated in the Sauerbrey equation, which is relative with the mass change per unit area at the QCM electrode surface to obtain change in oscillation frequency of the crystal [60].

$$\Delta f = -Cf \times \Delta m \tag{3.1}$$

where:

Δf = the observed frequency change in Hz,
Δm = the change in mass per unit area in μg^{-1} cm^2,
Cf = the sensitivity factor for the crystal (56.6 Hz μg^{-1} cm^2 for a 5 MHz AT-cut quartz crystal at RT).

The Sauerbrey equation works in order to a linear sensitivity factor, Cf, which is a fundamental property of the QCM crystal. As a result, in theory, the QCM mass sensor does not need calibration. However, the Sauerbrey equation is only strictly applicable to uniform, rigid, thin-film deposits. Vacuum and gas phase thin-film depositions, which are unsuccessful to require any of these conditions. Moreover, they confer more complicated frequency-mass correlations and often require some calibration to gain accurate results [57].

More recent developments have focused on modifying electrode surface chemistry (i.e. specialized polymer coatings [39], [53]. Due to that reason, these devices can be used as mass detectors for:

- specific gas detection,
- environmental monitoring,
- biosensing,
- basic surface-molecule interaction studies [57].

3.3.2 Water Contact Angle Measurements

This method is used to investigate wettability of substrate surfaces by contact of solid-water interface. Bare, activated, His-Silane SAM, Leu-Silane SAM, APTES modified SiO_2 surfaces and bare, activated, His-SH SAM, Leu-SH SAM, Ser-SH SAM, Trp-SH SAM modified Au substrates were measured with the aid of Aven Mighty Scope camera, USA and Image J image software. For each modified, activated and bare substrates, measurements were taken from 3 regions of each sample. Static surface angles of the drop placed on the surface were measured within 1min. After measurements, data were obtained from the software; J Image and water contact angle values were calculated [61].

3.4 Investigation of Protein Adsorption

Modified QCM crystals were investigated for protein adsorption via QCM. Human based albumin (Sigma Aldrich), fibrinogen from human plasma (Sigma Aldrich) and IgG (Sigma Aldrich and Ronsen Human IgG) were used to investigate adsorption behaviour. Phosphate buffered saline (PBS) Solution 7.4 pH (Sigma Aldrich) was used as buffer. 0.1mg/ml, 0.5mg/ml and 1mg/ml concentrations of the protein solutions were used. Before the investigation of protein adsorption, PBS buffer was passed through the system to remove the effect of Et-OH for ethanol soluble SAMs. Then, protein solutions were passed through the QCM flow cell system to observe change in frequency according to adsorption.

4. RESULTS

4.1 Characterization of Amino Acid Conjugated Self-Assembled Molecules

4.1.1 NMR Spectra of 3-(Trimethoxysilyl)propan Amino Acids [His-Si(OCH_3)]$_3$ and [Leu-Si(OCH_3)]$_3$

[His-Si(OCH_3)]$_3$ and [Leu-Si(OCH_3)]$_3$ were synthesized as described in section 3.1.1. First, Cbz-His-Bt intermediate was directly used for next reaction without any purification. For L-Leucine the oily reaction mixture was dissolved in ethylacetate and extracted using 20% aqueous solution of Na_2CO_3 to remove excess benzotriazole. Organic layer was dried over Na_2SO4 to give benzyl (1-(1H-benzo[d][1,2,3]triazol-1-yl)-4-methyl-1-oxopentan-2-yl) carbamate (Cbz-Leu-Bt) in 78% yield.

Cbz-His-Bt and Cbz-Leu-Bt were characterized by using NMR spectroscopy (Brueker, 500 MHz, Germany) in $CDCl_3$ or DMSO-d6. Tetramethysilane was used as internal standard.

^{1}H NMR (500 MHz, DMSO-d6) for Cbz-His-Bt from reaction mixture: δ = 9.13 (s, 1H), 8.54 (d, J = 7.2 Hz, 1H), 8.30 (q,J = 8.3 Hz, 2H), 7.82–7.87 (m, 1H),7.65–7.70 (m, 1H),7.54 (s, 1H), 7.30–7.37 (m, 5H), 5.88 (q, J = 8.3 Hz, 1H), 5.06 (s, 2H), 3.46–3.50 (m, 1H), 3.35–3.43 (m, 1H).

^{1}H-NMR (500 MHz, CDCl3) for Cbz-Leu-Bt, δ: 8.30 (d, J= 8.23 Hz, 1H), 8.15 (d, J= 8.23 Hz, 1H), 7.69 (t, J= 7.25 Hz, 1H), 7.55 (t, J= 7.25 Hz, 1H), 7.42-7.34 (m, 5H), 5.87 (dt, J= 8.29, 4.88 Hz, 1H), 5.51 (d, J= 8.49 Hz, 1H), 3.70 (s, 2H), 2.00-170 (m, 3H), 1.15 (d, J = 5.34 Hz, 3H), 1.00 (d, J = 5.34 Hz, 3H) ppm;

3-(trimethoxysilyl)propan-1-amine (1 eq.) was added drop wise to the solution of Cbz-AA-Bt (1 eq.) in CH_2Cl_2 under N_2 atmosphere at RT. Reaction was monitored by thin layer chromatography (TLC). After 30 minutes, reaction mixture was extracted using 10% Na_2CO3. Organic layer was dried over Na_2SO_4 to give Cbz-[His-Si(OCH_3)]$_3$ in 80% and Cbz-[Leu-Si(OCH_3)]$_3$ in 97 % yield.

^{1}H NMR (500 MHz, $CDCl_3$) for Cbz-[His-Si(OCH_3)]$_3$: = 10.3 (broad,s, 1H), 7.55 (s, 1H), 7.45-7.32 (m, 5H), 6.90 (s, 1H), 6.80 (s,1H), 5.15 (s, 2H), 4.55-4.45 (m, 1H), 3.85 (q, J= 6.90 Hz, 6H), 3.30-3.20 (m, 2H), 3.12 (broad, s, 1H), 2.98 (dd, J= 14,16, 5.00 Hz, 1H), 1.60-1.46 (m, 2H), 1.24 (t, J= 8.27 Hz, 9H), 0.50-0.40 (m, 2H) ppm.

^{1}H NMR (500 MHz, $CDCl_3$) for Cbz-[Leu-Si(OCH_3)]$_3$: = 7.42-7.35 (m, 5H), 6.25 (s, 1H), 5.30 (d, J= 8.18 Hz, 1H), 5.12 (s, 2H), 4.15 (dt, J= 8.29, 4.88 Hz, 1H), 3.85 (q, J= 6.98 Hz, 6H), 3.28 (dt, J= 11.92, 6.35Hz, 2H), 1.70-1.60 (m, 2H), 1.54 (p, J= 8.40 Hz, 2H), 1.24 (t, J= 6.98 Hz, 9H), 0.98-0.92 (m, 6H), 0.64 (t, J= 8.00 Hz, 2H) ppm.

[His-Si(OCH_3)]$_3$ and [Leu-Si(OCH_3)]$_3$ SAMs were obtained as white micro-crystals and in 91% yield and in 87% yield, respectively. ^{1}H NMR spectra of [His-Si(OCH_3)]$_3$ and [Leu-Si(OCH_3)]$_3$ SAM, were shown in Figure 4.1 and 4.2.

^{1}H NMR (500 MHz, $CDCl_3$) for [His-Si(OCH_3)] $_3$: = 10.2 (broad, s, 1H), 7.55 (s, 1H), 6.92 (s, 1H), 6.80 (s, 1H), 4.55-4.45 (m, 1H), 4.23 (broad, s, 2H), 3.85 (q, J= 6.90 Hz, 6H), 3.30-3.20 (m, 2H), 3.12 (broad, s, 1H), 2.98 (dd, J= 14,16, 5.00 Hz, 1H), 1.60-1.46 (m, 2H), 1.24 (t, J= 8.27 Hz, 9H), 0.50-0.40 (m, 2H) ppm.

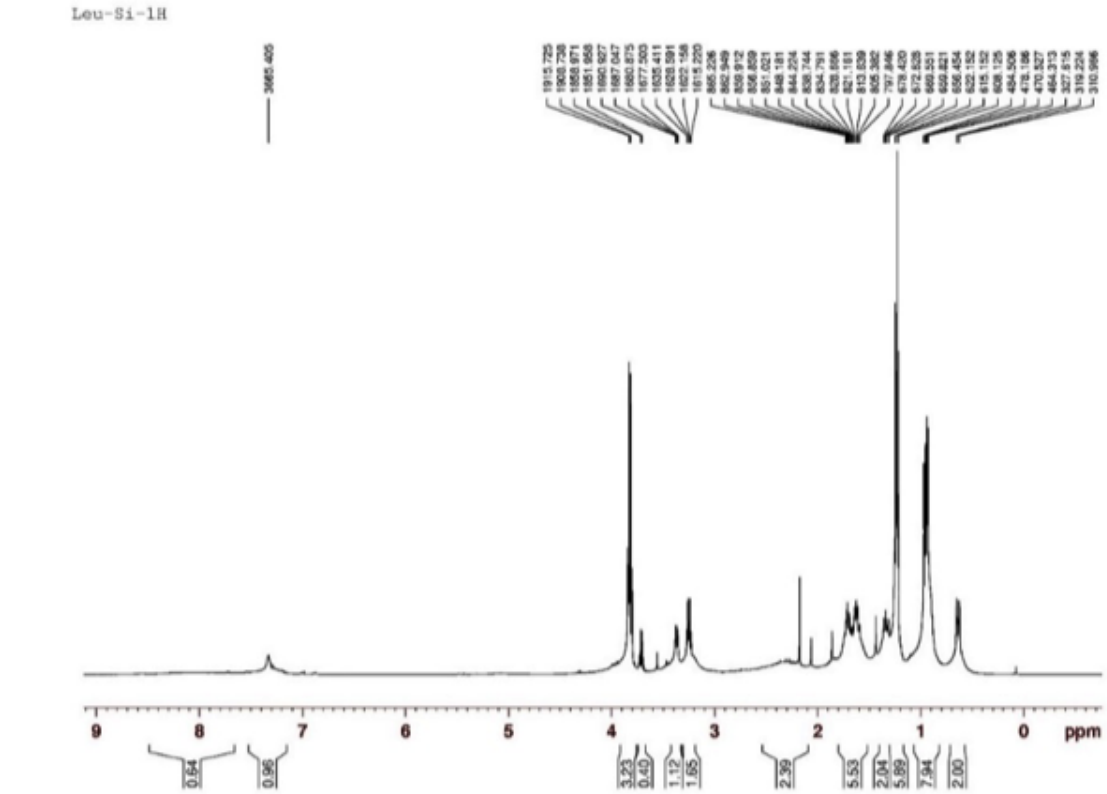

Figure 4.1 ^{1}H NMR spectrum of 2-Amino-3-(1H-imidazol-4-il)-N (3(triethoxysisily)propyl)pentane amide [His-Si(OCH_3)]$_3$ (4b).

^{1}H NMR (500 MHz, $CDCl_3$) for [Leu-Si(OCH_3)]$_3$: = 6.24 (s, 1H), 5.30 (d, J= 8.18 Hz, 1H), 4.25 (broad s, 2H), 4.15 (dt, J= 8.29, 4.88 Hz, 1H), 3.85 (q, J= 6.98 Hz, 6H), 3.28 (dt, J= 11.92, 6.35 Hz, 2H), 1.70-1.60 (m, 2H), 1.54 (p, J= 8.40 Hz, 2H), 1.24 (t, J= 6.98 Hz, 9H), 0.98-0.92 (m, 6H), 0.64 (t, J= 8.00 Hz, 2H) ppm.

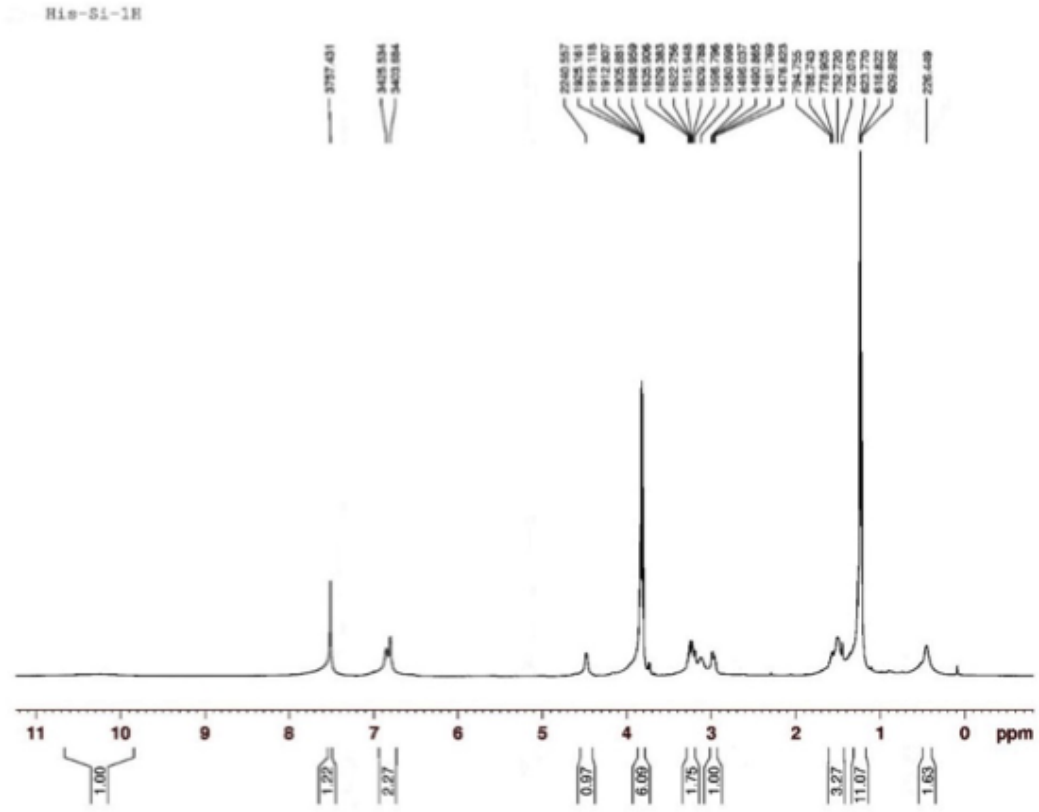

Figure 4.2 ^{1}H NMR spectrum of 2-Amino-4-methyl-N-(3(triethoxysisily)propyl)pentaneamide [Leu -Si$(OCH_3)]_3$.

4.1.2 NMR Spectra of 3-mercaptopropanoyl Amino Acids

- **NMR Spectrum of 3-(acetylthio)propanoic acid (2)**

Pyridine (3 eq.) was slowly added to the neat mixture of 3-mercaptopropionic acid, (1), (1 eq.) and acetic anhydride (3 eq.). The reaction mixture was allowed to stir overnight at RT. Reaction mixture was concentrated under vacuum, obtained crude mixture was dissolved in ether and washed with 0.5 N solution of KHSO4. The organic layers were collected and dried over Na_2SO4. Solvent was removed under vacuum to give 3-(acetylthio)propionic acid, (2) in 83% yield.

^{1}H NMR (500 MHz, $CDCl_3$) for 3-(acetylthio)propanoic acid: = 9,20 (s, br, 1H), 3.40 (t, J= 6.9 Hz, 2H), 2.72 (t, J= 6.9 Hz, 2H), 2.36 (s, 3H) ppm.

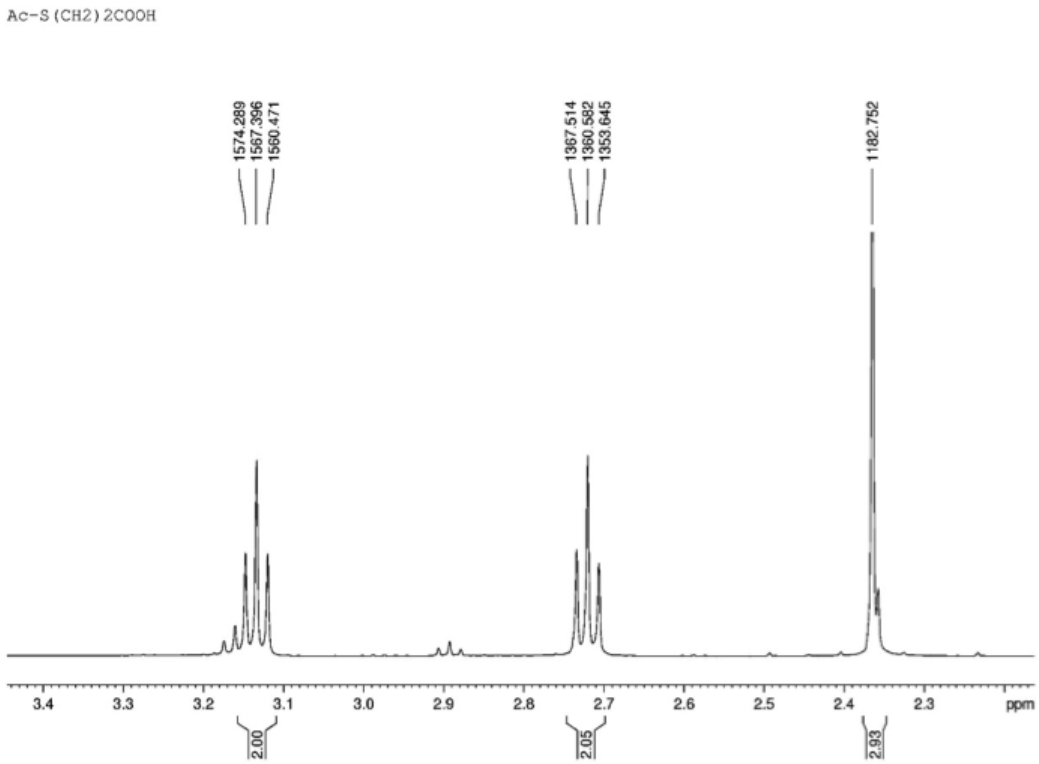

Figure 4.3 ^{1}H NMR Spectrum of 3-(acetylthio)propanoic acid.

• NMR Spectrum of S-(3-(1H-benzo [d][1,2,3]triazol-1-yl)- 3 -oxopropyl) ethanethioate (3)

Benzotriazole (BtH, 1 eq.) was added to the solution of 3-(acetylthio)propanoic acid, 2 (1 eq.) and DCC (1 eq.) in dry dichloromethane in ice bath. The reaction mixture was kept at this temperature for 16 h. The White precipitate was filtered off. Filtrate was extracted with 4N HCl. Organic layer was dried over Na_2SO4 and concentrated under vacuum to give S-(3-(1H-benzo[d][1,2,3]triazol-1-yl)-3-oxopropyl) ethanethioate, (3) in 80% yield.

^{1} H NMR (500 MHz, $CDCl_3$) for S-(3- (1H-benzo [d] [1,2,3] triazol-1-yl) -3-oxopropyl)

ethanethioate: = 8.32 (d, J= 8.3 Hz, 1H), 8.15 (d, J= 8.3 Hz, 1H), 7.70 (dt, J= 0.9; 7.15 Hz, 1H), 7.55 (dt, J= 0.9; 7.2 Hz, 1H), 3.80 (t, J= 6.8 Hz, 2H), 3.40 (t, J= 6.8 Hz, 2H), 2.40 (s, 3H) ppm.

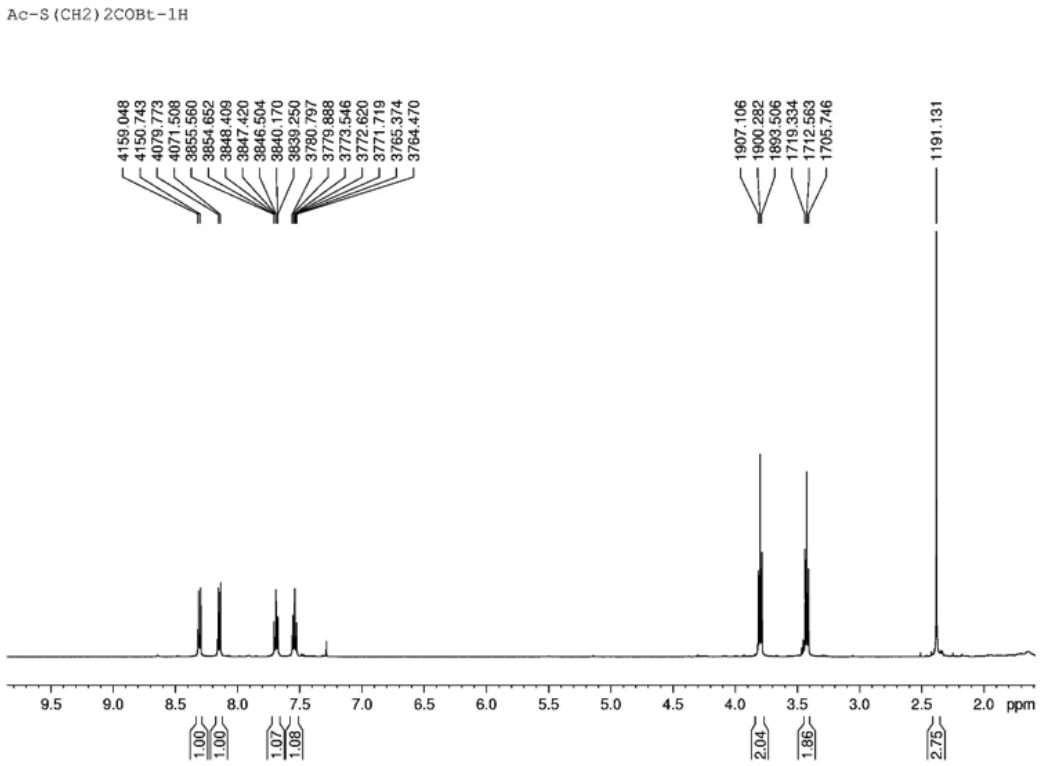

Figure 4.4 ^{1}H NMR spectrum of S-(3-(1H-benzo [d][1,2,3]triazol-1-yl)-3-oxopropyl) ethanethioate.

- **NMR Spectra of 3-mercaptopropanoyl Amino Acids (5)**

Amino acid (1 eq.) was dissolved in 1N NaOH (1.5 eq.) water solution. S-(3-(1H-benzo[d] [1,2,3]triazol-1-yl)-3-oxopropyl) ethanethioate, (3) (1 eq.) was added as an dioxane solution at RT. The reaction mixture was stirred at RT 30 min. Dioxane was removed under vacuum. The water solution was extracted with ethyl acetate to remove substituted 1H-benzotriazole. Water layer was acidified using 1N HCl. Water was removed, crude product was dissolved in EtOH and filtered. 4N HCl was added crude mixture and this mixture was refluxed for 3h to give 3-mercaptopropanoyl amino acids (5) in the yield between 78-89%. ^{1}H NMR spectra of 3-mercaptopropanoyl-histidine; 3-mercaptopropanoyl-leucine; 3-mercaptopropanoyl-serine; 3-mercaptopropanoyl- tryptophan were given in Figures 5-8, respectively.

^{1}H NMR for 3-mercaptopropanoyl-histidine (500 MHz, DMSO-d6) = 7.90 (s, 1H), 7.00 (s, 1H), 3.80-3.65 (m, 1H), 3.11 (dd, J= 4.7; 15.3 Hz, 1H), 2.94 (dd, J= 7.7; 28.3 Hz, 1H), 2.70-2.60 (m, 2H), 2.58-2.45 (m, 2H).

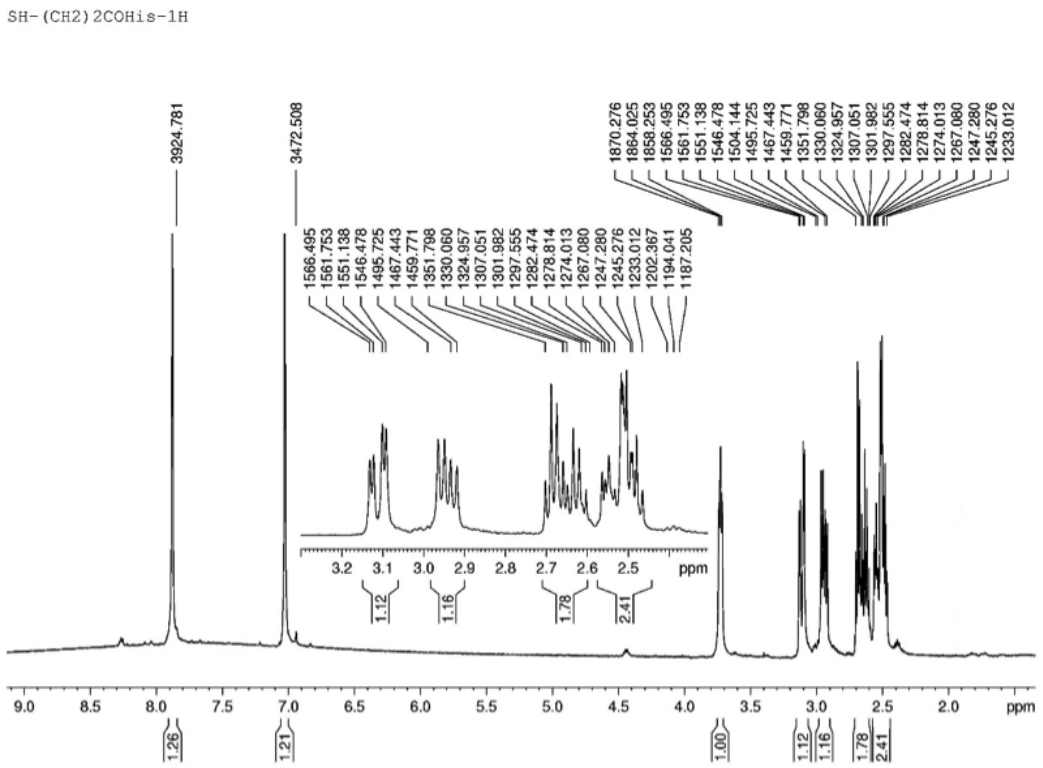

Figure 4.5 ^{1}H NMR spectrum of 3-mercaptopropanoyl-histidine.

^{1}H NMR for 3-mercaptopropanoyl-leucine (500 MHz, CDCl3) = 12.45 (s, br, 1H), 8.20 (d, J= 7.9 Hz, 1H), 4.30-4.10 (m, 1H), 3.10-2.90 (m, 2H), 2.45 (t, J= 7.0 Hz, 2H), 1.70-1.50 (m, 1H), 1.48-1.40 (m, 2H), 0.90 (d, J= 6.6 Hz, 3H), 0.70 (d, J= 6.6 Hz, 3H) ppm.

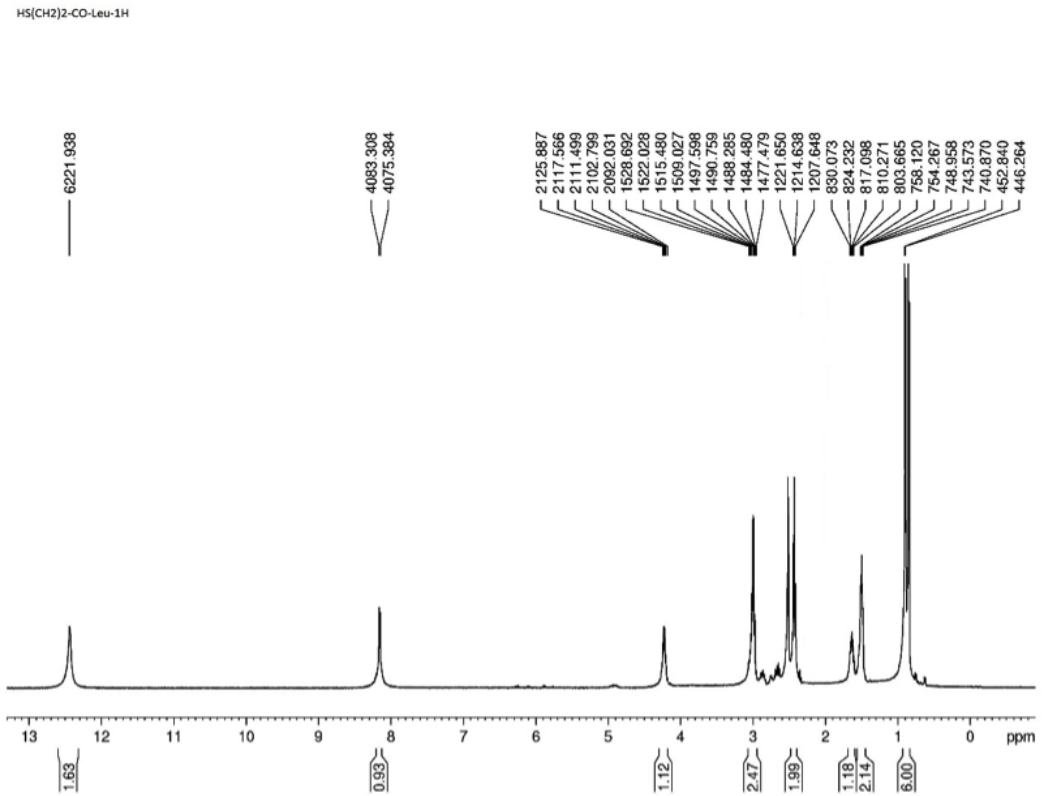

Figure 4.6 ^{1}H NMR spectrum of 3-mercaptopropanoyl-leucine.

^{1}H NMR for 3-mercaptopropanoyl-serine (500 MHz, CDCl3) = 12.39 (s, br, 1H), 8.32 (d, J= 7.9 Hz, 1H), 4.20 (m, 2H, -CH, -OH), 3.15 (m, 2H), 3.10 (dd, J= 4.7; 15.3 Hz, 1H), 2.90 (dd, J= 7.7; 28.3 Hz, 1H), 2.56-2.47 (m, 2H).

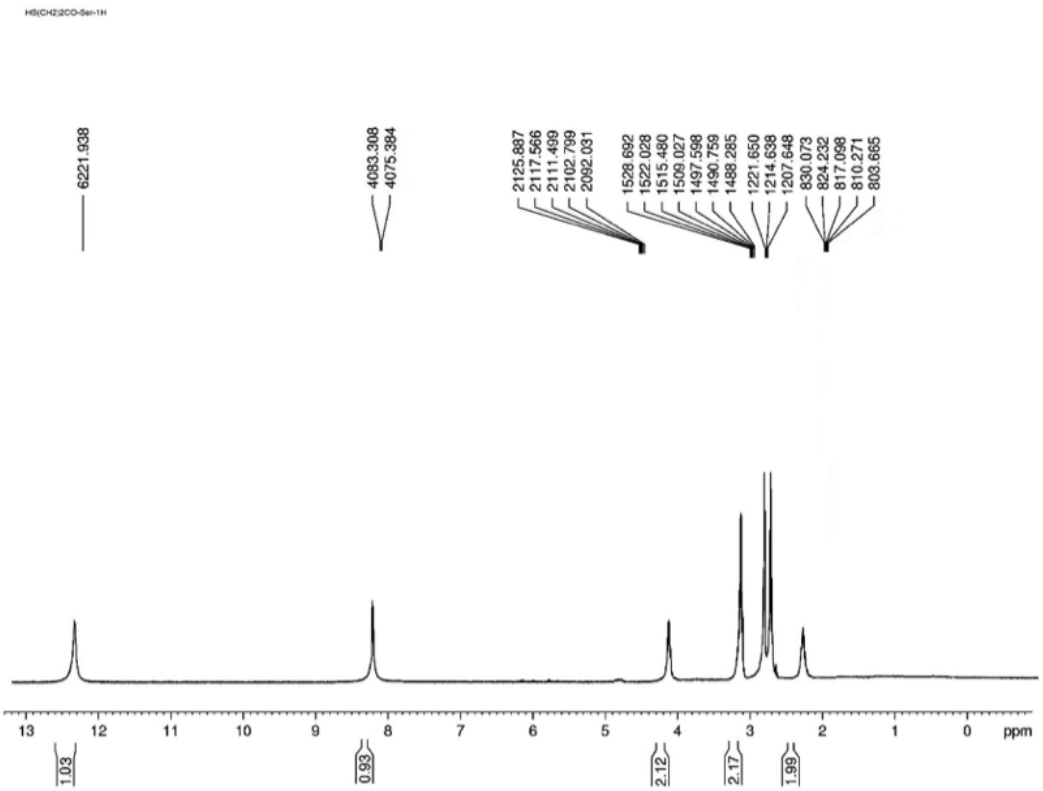

Figure 4.7 ^{1}H NMR spectrum of 3-mercaptopropanoyl-serine.

3-mercaptopropanoyl-tryptophan (500 MHz, $CDCl_3$) = 12.60 (s, br, 1H), 10.80 (s, 1H), 8.20 (d, J= 7.8 Hz, 1H), 7.50 (d, J= 7.8 Hz, 1H), 7.35 (d, J= 7.8 Hz, 1H), 7.15 (s, 1H), 7.10 (t, J= 7.40 Hz, 1H), 6.95 (t, J= 7.5 Hz, 1H), 4.50- 4.40 (m, 1H), 3.17 (dd, J= 5.0; 14.6 Hz, 1H), 3.10-2.90 (m, 3H), 2.50-2.30 (m, 2H) ppm.

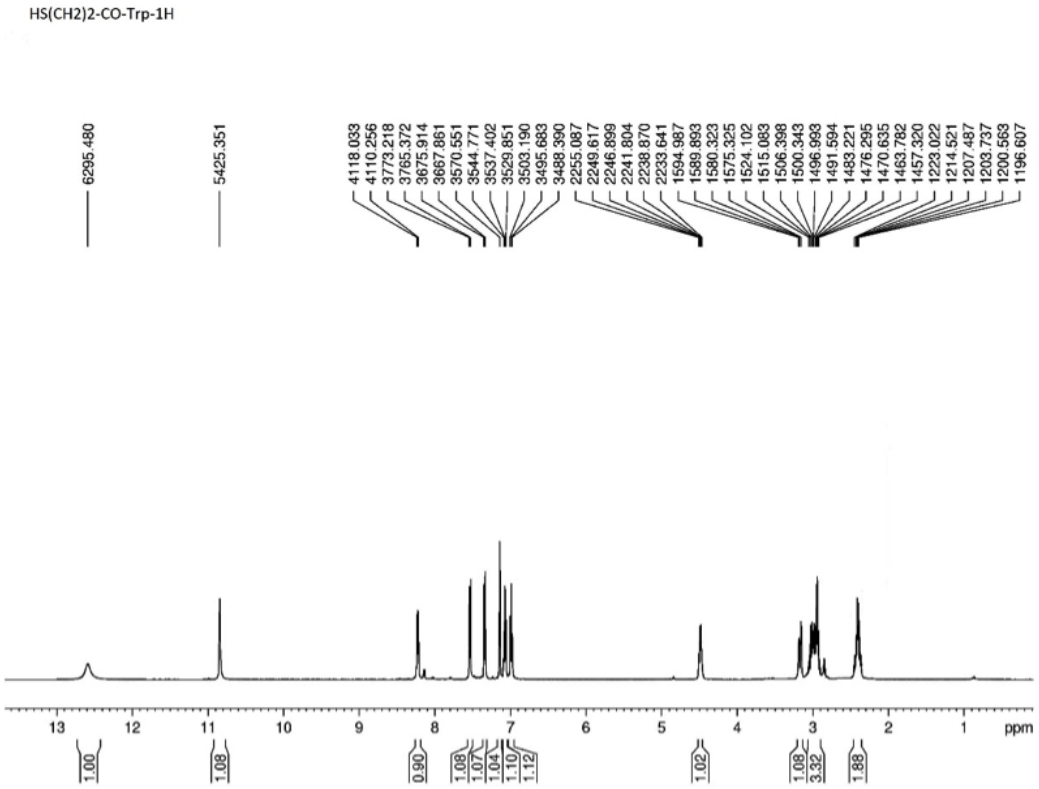

Figure 4.8 ^{1}H NMR for 3-mercaptopropanoyl-tryptophan.

4.1.3 QCM Analysis

His-SH SAM used as a reference to determine the optimum concentration of amino acid conjugated SAMs for in-situ surface modification of QCM crystals. 10-80mM (in absolute ethanol) His-SH solutions were used to modify Au QCM surfaces. The amount (in terms of mass) of immobilized SAMs was changed between 8.00-13.00 μg/cm^2. According to the measurements highest His-SH SAM immobilization was measured when 10mM SAM was used and found to be 13.00 μg/cm^2. From these results optimum concentration of solution was determined as 10mM and delta frequency and delta mass data were shown in Figure 4.9. 10mM SAM concentration was used for all other SAM in QCM experiments.

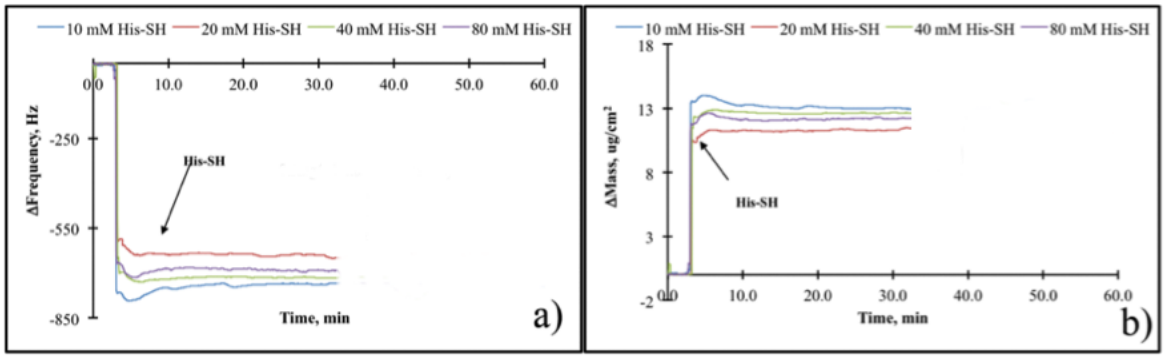

Figure 4.9 Effect of His-SH concentration on frequency and mass change in PBS pH:, 7.4 at RT.

Surface modification of all QCM crystals was investigated in-situ by QCM. The results are shown in Table 4.1 in terms of Δ frequency (Hz) and Δ mass (μg/cm^2).

Table 4.1
QCM results of SAM modifications.

Surface Modification 10mM	**Δ Frequency (Hz) (Average)**	**Δ Mass (μg/cm^2) (Average)**
His-Silane (on SiO_2)	566.36 ±34.59	10.3 ±1.9
Leu-Silane (on SiO_2)	545.12 ±26.11	10.2 ±1.6
APTES (on SiO_2)	559.59 ±41.15	10.1 ±1.1
His-SH (on Au)	797.10 ±144.91	13.5 ±0.6
Leu-SH (on Au)	757.92 ±31.37	13.5 ±0.6
Ser-SH (on Au)	701.50 ±19.80	12.2 ±0.4
Trp-SH (on Au)	676.24 ±48.90	12.1 ±2.5

4.1.4 Water Contact Angle Measurements

Water contact angle analysis of UV/Ozone treated, 10mM APTES, in situ 10mM amino acid conjugated SAM modified SiO_2 substrates were investigated. The results are shown in Table 4.2. UV/Ozone treated and bare SiO_2 substrates contact angle values were measured as 8.8°±0.6 ° and 35.8°±2.5 °, respectively. After APTES, His-Silane and Leu-Silane modification water contact angle values changed significantly to 28.2°±2.0 °, 49.6°±4.9 ° and 68.2°±0.3 °, respectively.

Table 4.2
Water contact angle results for SiO_2 crystal surfaces.

Substrates	**Contact Angle (°)**
Bare SiO_2	35.8 ±2.5
UV/Ozone Treated SiO_2	8.8 ±0.6
10mM His-Silane SAM modified	49.6 ±4.9
10mM Leu-Silane SAM modified	68.2 ±0.3
10mM APTES modified	28.2±2.0

Water contact angle analysis of UV/Ozone treated, 10mM APTES, in situ 10mM amino acid conjugated SAM modified Au substrates were also investigated. Water contact angle values of UV/Ozone treated Au and bare Au substrates (after UV/Ozone treatment Au substrates were immersed in absolute ethanol for 1 hour) were measured to be 26.5°±6.7 ° and 61.9°±9.3 °, respectively. Water contact angle results of Au crystal surfaces were shown in Table 4.3. Amino acid conjugated (histidine, leucine, serine and tryptophan) have shown no significant difference in water contact angle values after modification as 65.3°±2.7 °, 63.9°±4.3 °, 70.4°±1.4 °, 69.0°±1.3 °, respectively.

Table 4.3
Contact angle results for Au crystal surfaces.

Substrates	**Contact Angle (°)**
UV/Ozone Treated Au	26.5 ±6.7
Bare Au	61.9 ±9.3
His-SH	65.3 ±2.7
Leu-SH	63.9 ±4.3
Ser-SH	69.0 ±1.3
Trp-SH	70.4 ±1.3

4.2 Protein Adsorption Analysis

4.2.1 Non-specific Protein Adsorption

Non-specific protein adsorption to amino acid conjugated SAM modified SiO_2 and Au substrates were investigated in-situ by QCM sensor. To compose control groups, protein adsorption to bare SiO_2 and Au substrates were investigated with 0.5mg/ml target proteins (albumin, fibrinogen and IgG solutions). Delta frequency (Hz) and delta mass (μg/cm^2) data were given in Figure 4.10 and Figure 4.11.

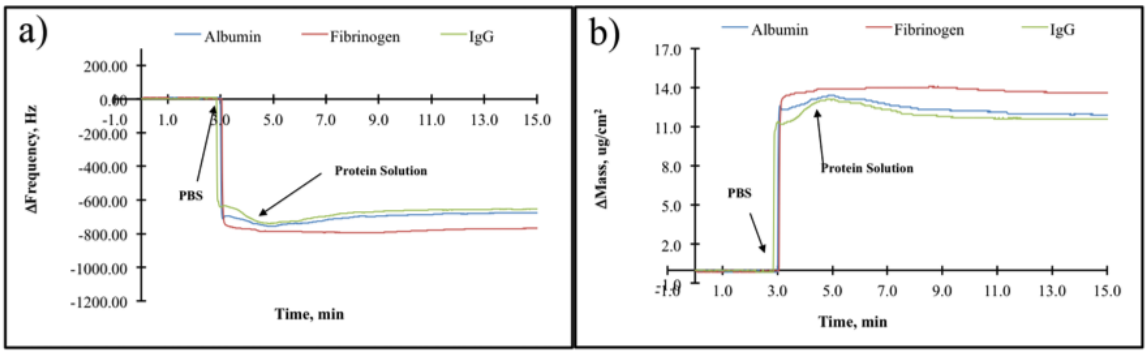

Figure 4.10 Non-specific protein adsorption to bare SiO_2 surface; Δ frequency in Hz and b is Δ mass results. Albumin, Fibrinogen and IgG concentration (0.5mg/ml) in PBS: 7.4 at RT.

According to the delta mass values, protein adsorption on bare SiO_2 surface Fibrinogen has shown the highest and IgG has shown the lowest affinity and mass values decreases as follows; Fibrinogen (13.80 μg/cm^2) > Albumin (11.70 g/cm^2)> IgG (11.16 μg/cm^2).

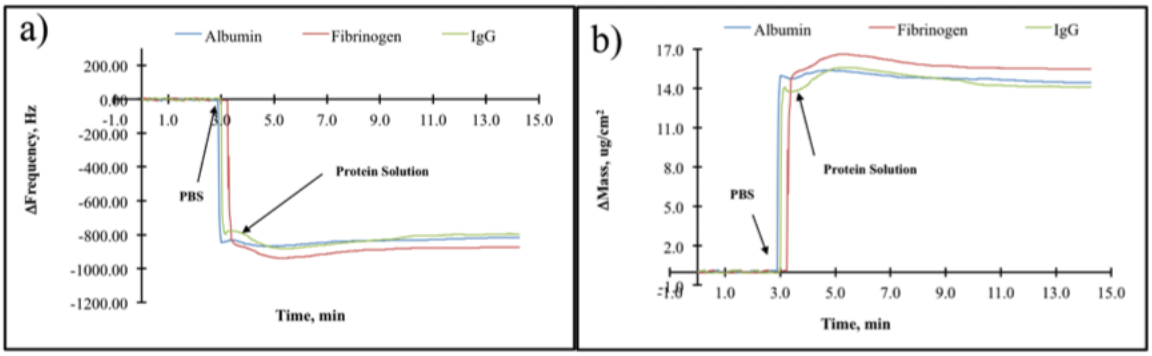

Figure 4.11 Non-specific protein adsorption to bare Au surface; Δ frequency in Hz and b is Δ mass results. Albumin, Fibrinogen and IgG concentration (0.5mg/ml) in PBS: 7.4 at RT.

According to the Δ mass values, protein adsorption on bare Au surface Fibrinogen has shown highest and IgG has shown the lowest affinity and mass values decreases as follows; Fibrinogen (15.52 $\mu g/cm^2$) > Albumin (14.60 $\mu g/cm^2$) > IgG (14.10 $\mu g/cm^2$).

Similar protein adsorption behavior was observed for both SiO_2 and Au surfaces. However, more proteins adsorbed non-specific to Au surfaces when compared to SiO_2.

The effect of protein concentration on non-specific adsorption were investigated and three different concentration of target proteins (albumin, fibrinogen and IgG) adsorption were carried out on bare Au surfaces. The results were shown in Figure 4.12 in terms of Δ frequency (Hz) and Δ mass ($\mu g/cm^2$).

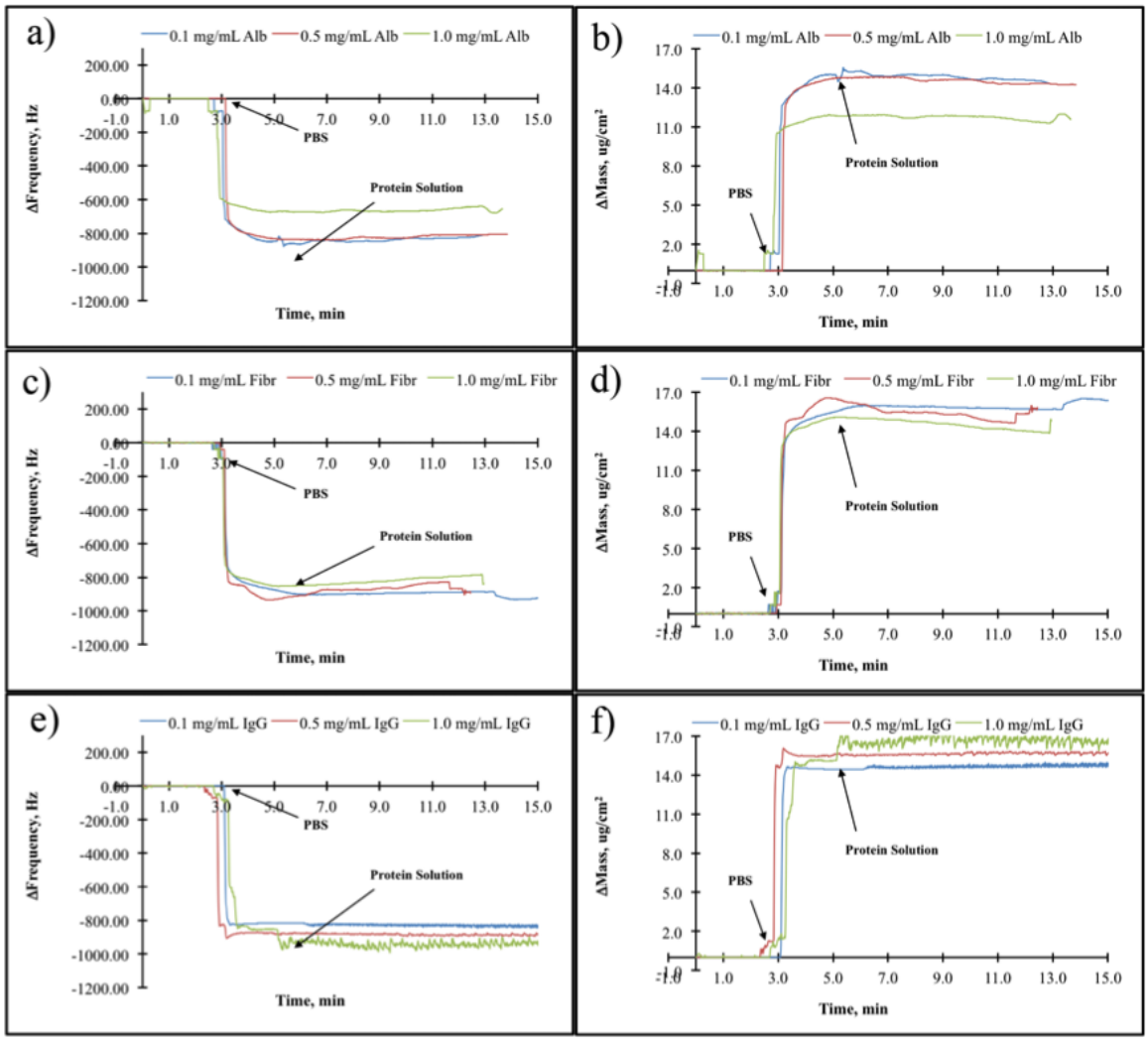

Figure 4.12 Effect of concentration on non-specific protein adsorption to bare Au surface; a and b Δ frequency Δ mass results for albumin; c and d for fibrinogen; e and f for IgG adsorption in PBS: 7.4 at RT, protein concentrations (0.1-1.0 mg/ml).

Albumin at 0.1 and 0.5 mg/ml concentrations has shown similar protein adsorption in terms of mass (14.83 and 14.64 $\mu g/cm^2$) and at the highest concentration (1.0 mg/ml, 11.80 $\mu g/cm^2$) fewer Albumin was adsorbed to Au surface. Similar adsorption profile was observed for fibrinogen and mass changes were measured as follows; 15.80 $\mu g/cm^2$, 15.25 $\mu g/cm^2$ and 14.24 $\mu g/cm^2$ for 0.1 mg/ml, 0.5 mg/ml and 1.0 mg/ml, respectively. IgG non-specific adsorption has shown different profile than the albumin and fibrinogen that highest adsorption was measured at 1.0 mg/ml protein concentration. Δ mass values were measured as follows; 14.55 $\mu g/cm^2$, 15.72 $\mu g/cm^2$ and 16.75 $\mu g/cm^2$ for 0.1 mg/ml, 0.5 mg/ml and 1.0 mg/ml, respectively.

4.2.2 Protein Adsorption Results on His-Silane Modified SiO_2 Surfaces

Protein adsorption to 10mM His-Silane SAM modified SiO_2 surfaces were investigated by QCM. The concentrations of target proteins (albumin, fibrinogen and IgG) were prepared between 0.1-1mg/ml in PBS. Protein adsorptions results were shown in Figure 4.13.

Fibrinogen has shown the highest affinity and mass change at all protein concentrations on Leu-Silane modified SiO_2 surfaces as 4.70 $\mu g/cm^2$, 7.80 $\mu g/cm^2$, and 19.20 $\mu g/cm^2$, respectively. For all proteins, increasing the protein concentration resulted with increased mass change on Leu-Silane modified SiO_2 surfaces. For albumin, delta mass values were measured as follows; 1.83 $\mu g/cm^2$, 5.24 $\mu g/cm^2$ and 8.38 $\mu g/cm^2$ for 0.1 mg/ml, 0.5 mg/ml and 1.0 mg/ml, respectively. For IgG, delta mass values were measured as follows; 2.20 $\mu g/cm^2$, 6.40 $\mu g/cm^2$ and 6.90 $\mu g/cm^2$ for 0.1 mg/ml, 0.5 mg/ml and 1.0 mg/ml, respectively and were shown in Table 4.4. For all proteins, increasing the protein concentration resulted with increased mass change on His-Silane modified SiO_2 surfaces.

Table 4.4
Δ Frequency and Δ mass results of protein adsorption on His-Silane Modified SiO_2 surfaces.

His-Silane	**Δ Frequency (Hz)**			**Δ Mass ($\mu g/cm^2$)**		
Proteins	**0.1mg/ml**	**0.5mg/ml**	**1mg/ml**	**0.1mg/ml**	**0.5mg/ml**	**1mg/ml**
Albumin	153.90	289.50	471.80	1.83	5.24	8.38
Fibrinogen	267.40	455.50	926.70	4.70	7.80	19.20
IgG	102.20	345.00	359.90	2.20	6.40	6.90

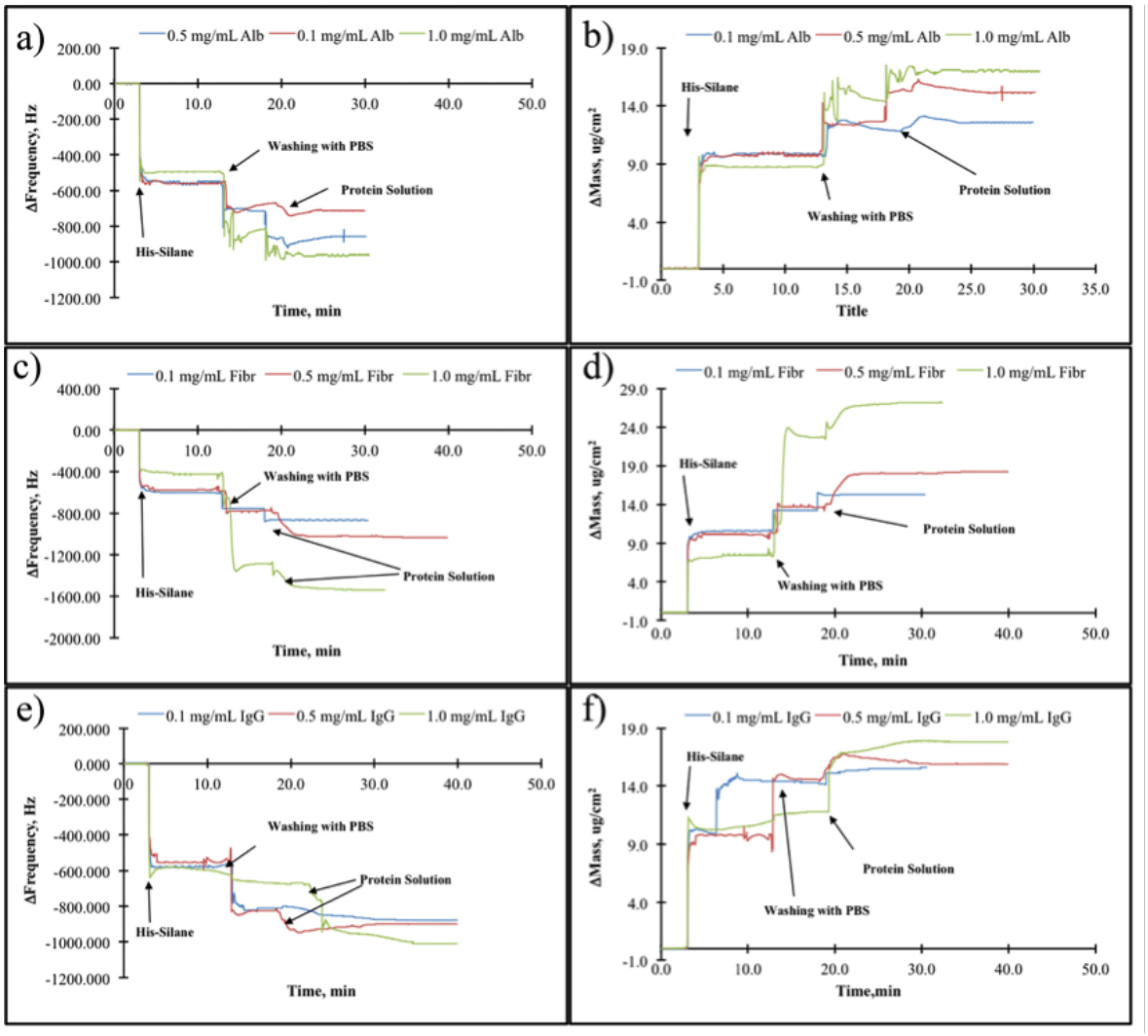

Figure 4.13 Protein adsorption results of 10mM His-Silane modified SiO_2 surfaces. a, c, and e are Δ frequency results (Hz). b, d and f are the Δ mass results ($\mu g/cm^2$) of protein adsorption in PBS: 7.4 at RT.

4.2.3 Protein Adsorption on Leu-Silane Modified SiO_2 Surfaces

Protein adsorption to 10mM Leu-Silane SAM modified SiO_2 surfaces were investigated by QCM. The concentrations of target proteins (albumin, fibrinogen and IgG) were prepared between 0.1-1mg/ml in PBS. Protein adsorptions results were shown in Figure 4.14.

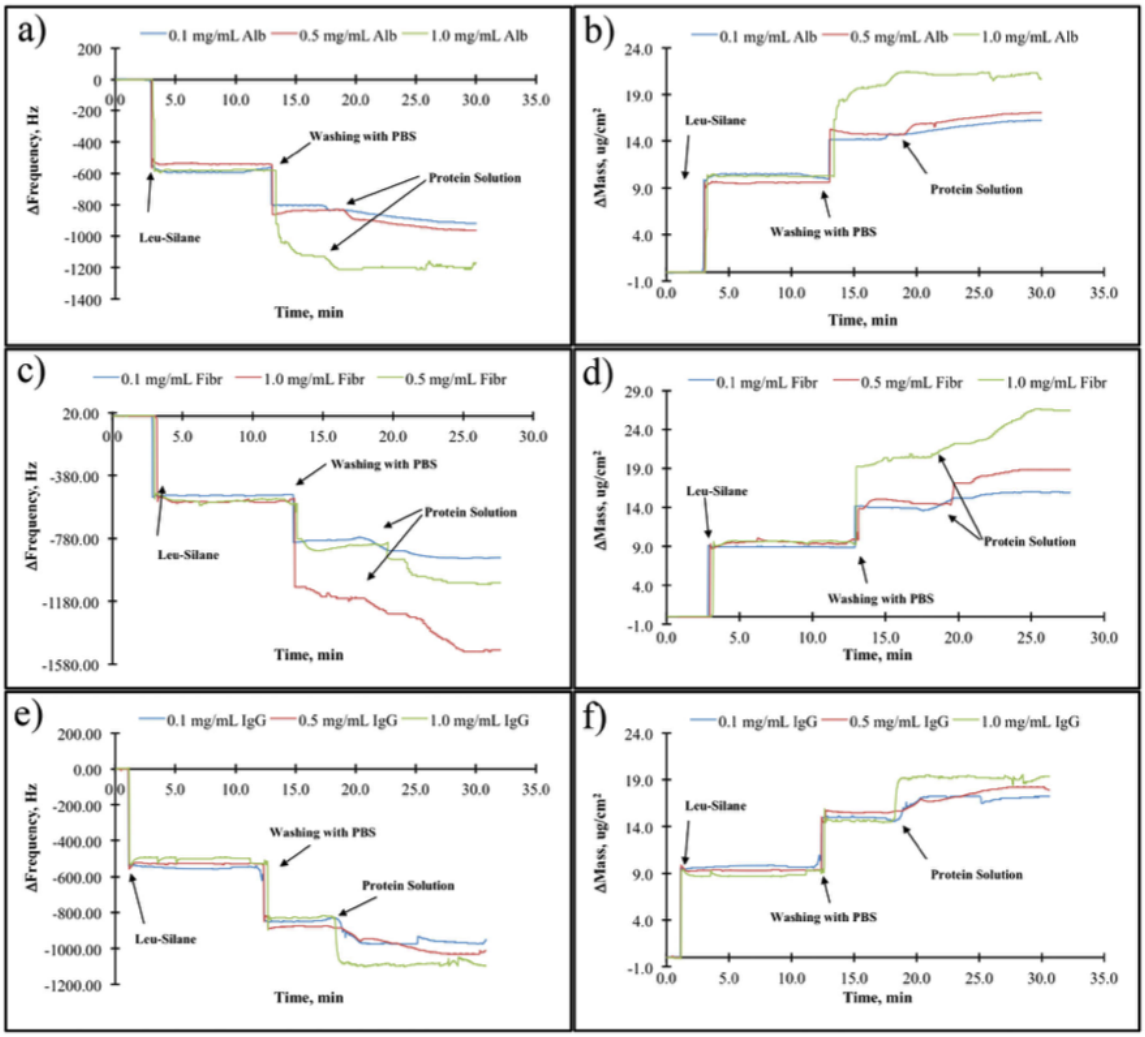

Figure 4.14 Protein adsorption results of 10mM Leu-Silane modified SiO_2 surfaces. a, c, and e are Δ frequency results (Hz). b, d and f are the Δ mass results ($\mu g/cm^2$) of protein adsorption in PBS: 7.4 at RT.

Table 4.5
Δ Frequency and Δ mass results of protein adsorption on 10mM Leu-Silane Modified SiO_2 surfaces.

Leu Silane	**Δ Frequency (Hz)**			**Δ Mass (μg/cm^2)**		
Proteins	**0.1mg/ml**	**0.5mg/ml**	**1mg/ml**	**0.1mg/ml**	**0.5mg/ml**	**1mg/ml**
Albumin	376.00	409.21	607.00	5.70	6.70	11.40
Fibrinogen	397.00	518.00	965.00	7.10	9.10	16.80
IgG	453.60	483.20	595.90	7.20	8.90	10.60

IgG has shown the highest affinity and mass change to at 0.1 mg/ml concentration, while Fibrinogen has shown the highest affinity to at 0.5 and 1.0 mg/ml concentrations on Leu-Silane modified SiO_2 surfaces as 7.20 μg/cm^2, 9.10 μg/cm^2, and 16.80 μg/cm^2, respectively. For all proteins, increasing the protein concentration resulted with increased mass change on Leu-Silane modified SiO_2 surfaces. For albumin, Δ mass values were measured as follows; 5.70 μg/cm^2, 6.70 μg/cm^2 and 11.40 μg/cm^2 for 0.1 mg/ml, 0.5 mg/ml and 1.0 mg/ml, respectively. For fibrinogen, Δ mass values were measured as follows; 7.10 μg/cm^2, 9.1μg/cm^2 and 16.80 μg/cm^2 for 0.1 mg/ml, 0.5 mg/ml and 1.0 mg/ml, respectively. For IgG, delta mass values were measured as follows; 7.20 μg/cm^2, 8.90 μg/cm^2 and 10.6 μg/cm^2 for 0.1 mg/ml, 0.5 mg/ml and 1.0 mg/ml, respectively and were shown in Table 4.5.

4.2.4 Protein Adsorption on APTES Modified SiO_2 Surfaces

Protein adsorption to 10mM APTES SAM modified SiO_2 surfaces were investigated by QCM. The concentrations of target proteins (albumin, fibrinogen and IgG) were prepared between 0.1-1mg/ml in PBS. Protein adsorptions results were shown in Figure 4.15.

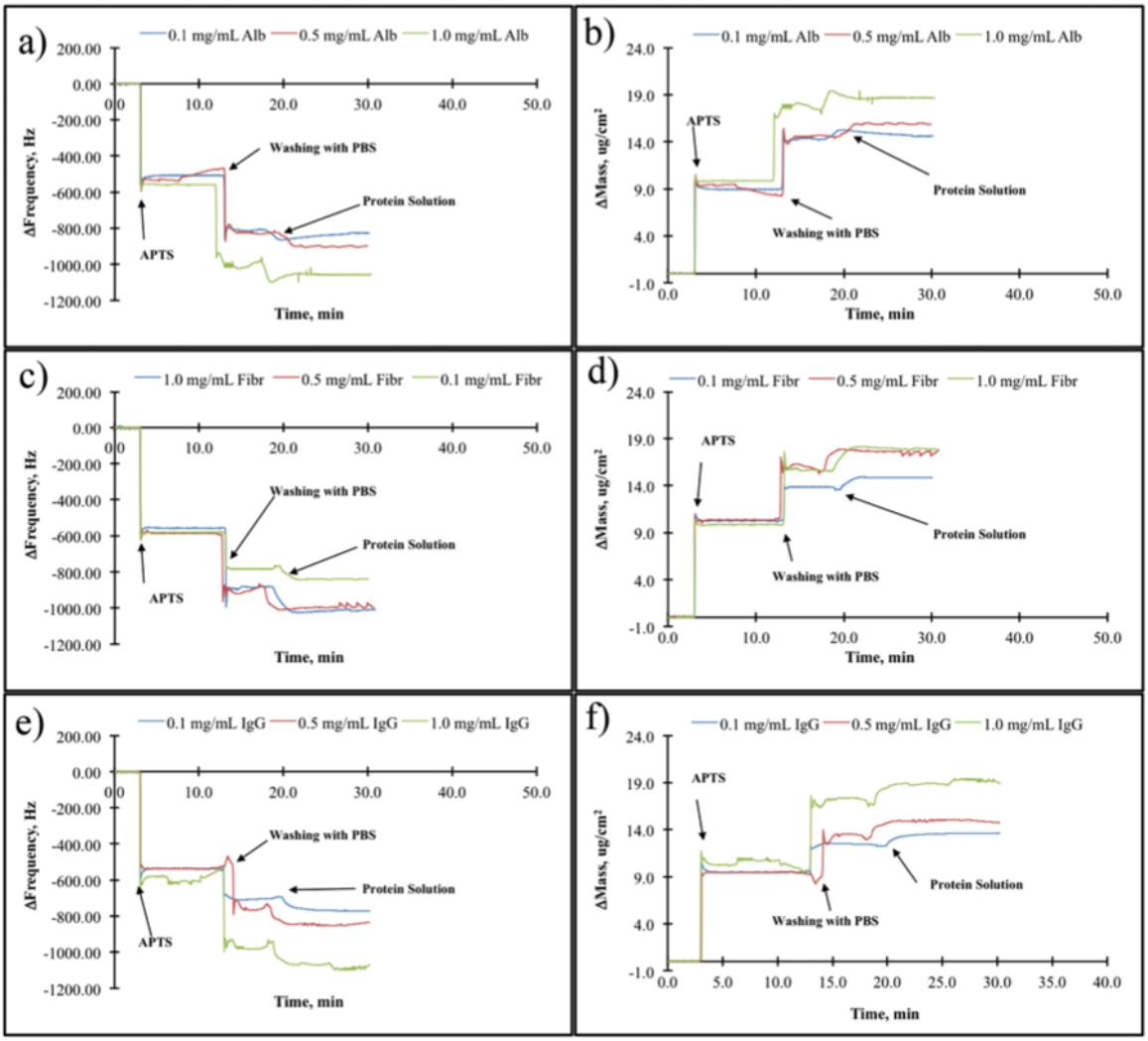

Figure 4.15 Protein adsorption results of 10mM APTES modified SiO_2 surfaces. a, c, and e are Δ frequency results (Hz). b, d and f are the Δ mass results ($\mu g/cm^2$) of protein adsorption in PBS: 7.4 at RT.

To investigate the effect of a conventional SAM molecule APTES was chosen. Fibrinogen has shown the highest affinity and mass change to at 0.1 and 0.5 mg/ml concentrations, while Albumin has shown the highest affinity to at 0.5 and 1.0 mg/ml concentrations on APTES modified SiO_2 surfaces as 8.00 $\mu g/cm^2$, 7.30 $\mu g/cm^2$, and 8.80 $\mu g/cm^2$, respectively. For albumin and IgG, increasing the protein concentration resulted with increased mass change on APTES modified SiO_2 surfaces. However for Fibrinogen increasing the protein concentration resulted with decreased mass change. For albumin, delta mass values were measured as follows; 5.80 $\mu g/cm^2$, 6.90 $\mu g/cm^2$ and 8.80 $\mu g/cm^2$ for 0.1 mg/ml, 0.5 mg/ml and 1.0 mg/ml, respectively. For fibrinogen, delta mass values were measured as follows; 8.00 $\mu g/cm^2$, 7.30 $\mu g/cm^2$ and 5.00 $\mu g/cm^2$ for 0.1 mg/ml, 0.5 mg/ml and 1.0 mg/ml, respectively. For IgG, delta mass values were measured as follows; 4.00 $\mu g/cm^2$, 4.70 $\mu g/cm^2$ and 8.40 $\mu g/cm^2$ for 0.1 mg/ml, 0.5 mg/ml and 1.0 mg/ml, respectively and were shown in Table 4.6.

Table 4.6
Δ Frequency and Δ mass results of protein adsorption on APTES Modified SiO_2 surfaces.

APTES	**Δ Frequency (Hz)**			**Δ Mass ($\mu g/cm^2$)**		
Proteins	**0.1mg/ml**	**0.5mg/ml**	**1mg/ml**	**0.1mg/ml**	**0.5mg/ml**	**1mg/ml**
Albumin	328.00	366.70	498.10	5.80	6.90	8.80
Fibrinogen	259.90	405.80	435.50	8.00	7.30	5.00
IgG	244.60	314.10	482.30	4.00	4.70	8.40

4.2.5 Protein Adsorption on His-SH Modified Au Surfaces

Protein adsorption to 10mM His-SH SAM modified Au surfaces were investigated by QCM. The concentrations of target proteins (albumin, fibrinogen and IgG) were prepared between 0.1-1mg/ml in PBS. Protein adsorptions results were shown in Figure 4.16.

No mass change was observed on His-SH modified Au surfaces when Albumin was used at all protein concentrations. Fibrinogen has shown the lowest affinity and mass change to at 0.5 and 1.0 mg/ml concentrations, while IgG has shown similiar

Table 4.7
Δ Frequency and Δ mass results of protein adsorption on His-SH Modified Au surfaces.

10mM His-SH	**Δ Frequency (Hz)**			**Δ Mass (μg/cm^2)**		
Proteins	**0.1mg/ml**	**0.5mg/ml**	**1mg/ml**	**0.1mg/ml**	**0.5mg/ml**	**1mg/ml**
Albumin	328.00	366.70	498.10	5.80	6.90	8.80
Fibrinogen	259.90	405.80	435.50	8.00	7.30	5.00
IgG	244.60	314.10	482.30	4.00	4.70	8.40

affinity at 0.5 and 1.0 mg/ml concentrations to His-SH modified Au surfaces as 1.40 μg/cm^2, 2.20 μg/cm^2, and 0.90 μg/cm^2, respectively. For Fibrinogen, increasing the protein concentration resulted with increased mass change on His-SH modified Au surfaces. Results were shown in Table 4.7

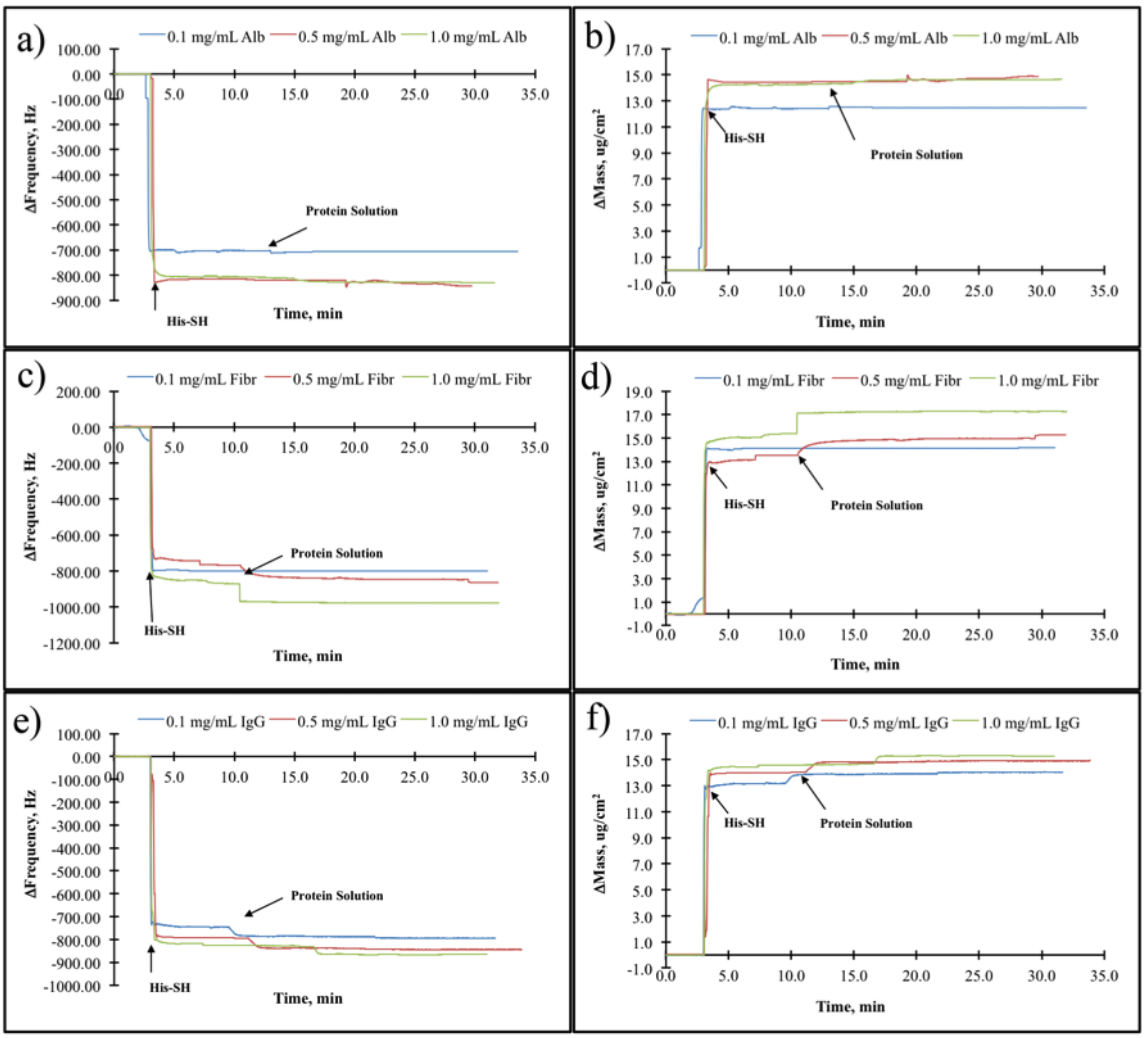

Figure 4.16 Protein adsorption results of 10mM His-SH modified Au surface; a, c, and e are Δ frequency results (Hz); b, d and f are the Δ mass results ($\mu g/cm^2$) of protein adsorption in PBS: 7.4 at RT.

4.2.6 Protein Adsorption Results on Leu-SH SAM Modified Au Surfaces

Protein adsorption to 10mM Leu-SH SAM modified Au surfaces were investigated by QCM. The concentrations of target proteins (albumin, fibrinogen and IgG) were prepared between 0.1-1mg/ml in PBS. Protein adsorptions results were shown in Figure 4.17.

IgG has shown the highest affinity and mass change to at 0.1 mg/ml concentration, while Fibrinogen has shown the highest affinity to at 0.5 and 1.0 mg/ml concentrations on Leu-SH modified Au surfaces as 8.50 μg/cm^2, 8.70 μg/cm^2, and 16.60 μg/cm^2, respectively. Only for Fibrinogen, increasing the protein concentration resulted with increased mass change on Leu-SH modified Au surfaces. For Albumin and IgG amount of adsorbed protein decreased at 0.5 mg/ml and increased and reached the highest amount at 1.0 mg/ml concentration. For Albumin Δ mass values were measured as follows; 5.60 μg/cm^2, 2.50 μg/cm^2 and 11.30 μg/cm^2 for 0.1 mg/ml, 0.5 mg/ml and 1.0 mg/ml, respectively. For IgG, Δ mass values were measured as follows; 8.50 μg/cm^2, 7.90 μg/cm^2 and 8.30 μg/cm^2 for 0.1 mg/ml, 0.5 mg/ml and 1.0 mg/ml, respectively and were shown in Table 4.8.

Table 4.8
Δ Frequency and Δ mass results of protein adsorption on Leu-SH Modified Au surfaces.

10mM Leu-SH	**Δ Frequency (Hz)**			**Δ Mass (μg/cm^2)**		
Proteins	**0.1mg/ml**	**0.5mg/ml**	**1mg/ml**	**0.1mg/ml**	**0.5mg/ml**	**1mg/ml**
Albumin	319.40	139.00	624.30	5.60	2.50	11.30
Fibrinogen	394.60	534.20	944.40	7.10	8.70	16.60
IgG	473.90	447.02	472.00	8.50	7.90	8.30

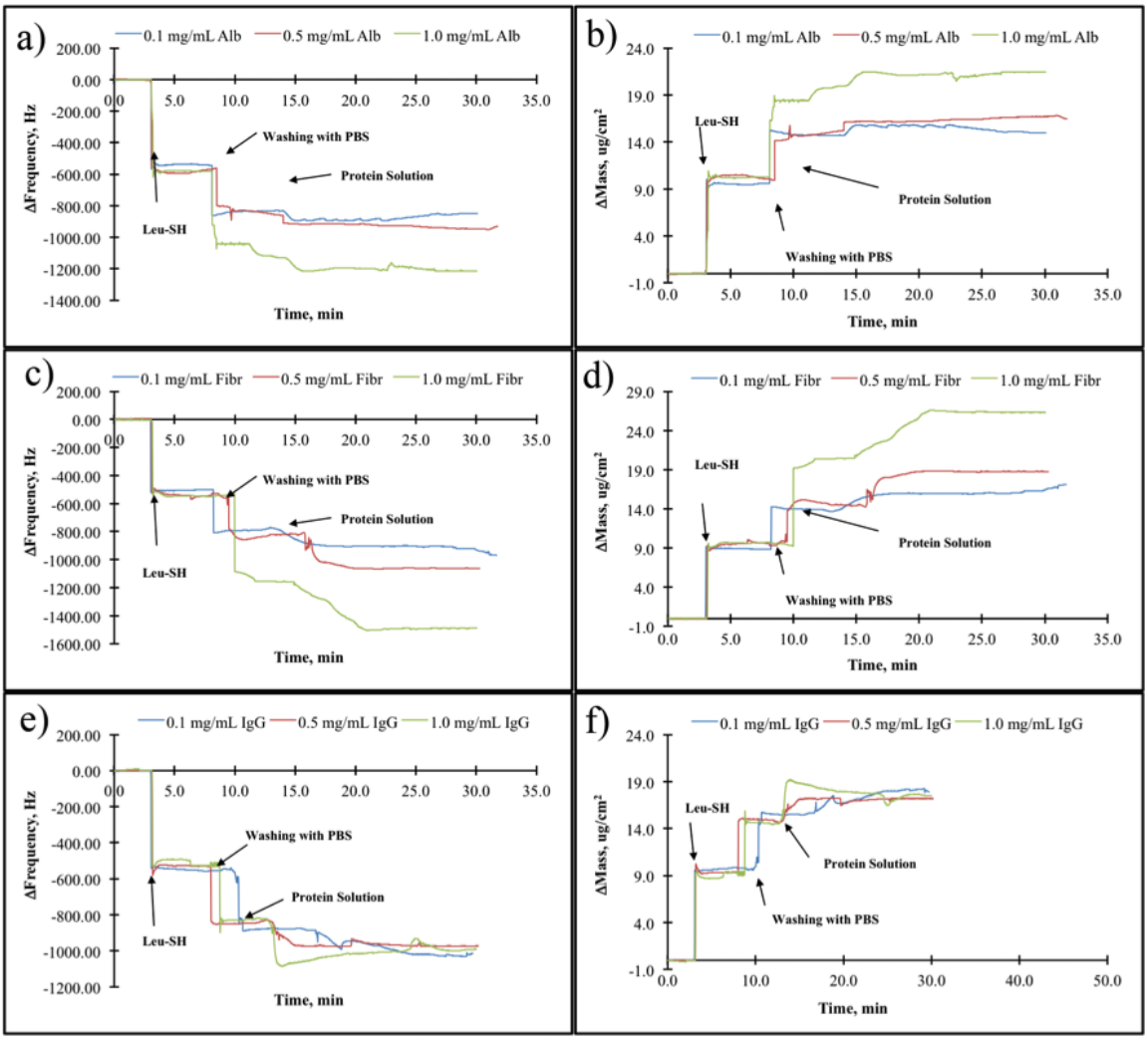

Figure 4.17 Protein adsorption results of 10mM Leu-SH modified Au surface; a, c, and e are Δ frequency results (Hz); b, d and f are the Δ mass results (μg/cm^2) of protein adsorption in PBS: 7.4 at RT.

4.2.7 Protein Adsorption on Ser-SH Modified Au Surfaces

Protein adsorption to 10mM Ser-SH SAM modified Au surfaces were investigated by QCM. The concentrations of target proteins (albumin, fibrinogen and IgG) were prepared between 0.1-1mg/ml in PBS. Protein adsorptions results were shown in Figure 4.18.

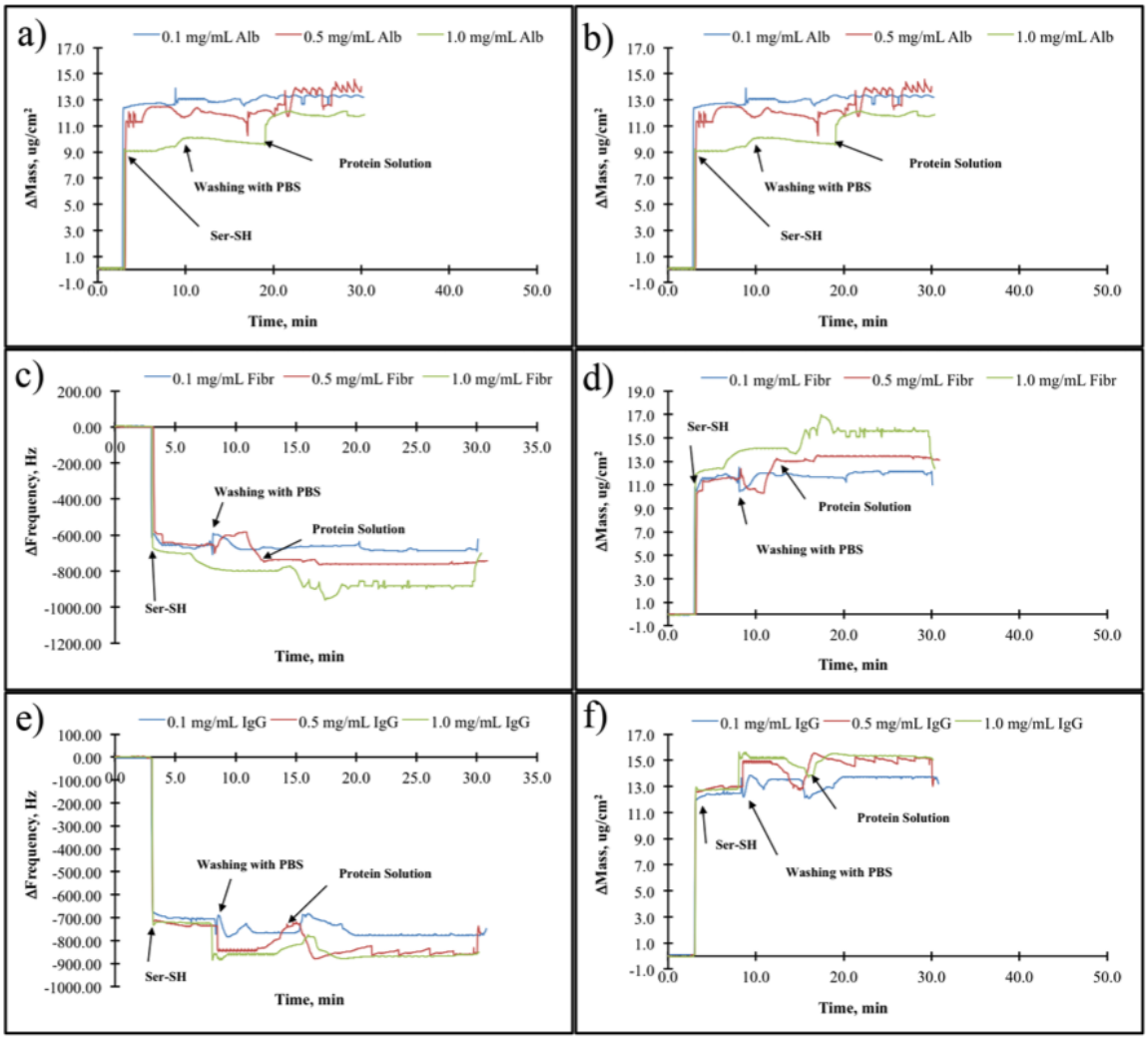

Figure 4.18 Protein adsorption results of 10mM Ser-SH modified Au surface; a, c, and e are Δ frequency results (Hz); b, d and f are the Δ mass results (μg/cm^2) of protein adsorption in PBS: 7.4 at RT.

No mass change was observed on Ser-SH modified Au surfaces at concentration of 0.1 mg/ml in proteins. Fibrinogen has shown the highest affinity and mass change to at 0.5 and 1.0 mg/ml concentrations, while IgG has shown the lowest affinity at 0.5 and 1.0 mg/ml concentrations to Ser-SH modified Au surfaces as 1.90 μg/cm^2, 3.30 μg/cm^2, and 0.30 μg/cm^2 and 2.30 μg/cm^2, respectively. For Albumin Δ mass values were measured as follows; 1.40 μg/cm^2 and 3.30 μg/cm^2 for 0.5 mg/ml and 1.0 mg/ml, respectively. For all proteins, increasing the protein concentration resulted with increased mass change on Ser-SH modified Au surfaces. Results were shown in Table 4.9.

Table 4.9
Δ Frequency and Δ mass results of protein adsorption on Ser-SH Modified Au surfaces.

10mM Ser-SH	**Δ Frequency (Hz)**			**Δ Mass (μg/cm^2)**		
Proteins	**0.1mg/ml**	**0.5mg/ml**	**1mg/ml**	**0.1mg/ml**	**0.5mg/ml**	**1mg/ml**
Albumin	None	71.30	152.90	None	1.40	2.70
Fibrinogen	None	121.90	206.10	None	1.90	3.30
IgG	None	112.00	124.90	None	0.30	2.30

4.2.8 Protein Adsorption on Trp-SH Modified Au Surfaces

Protein adsorption to 10mM Trp-SH SAM modified Au surfaces were investigated by QCM. The concentrations of target proteins (albumin, fibrinogen and IgG) were prepared between 0.1-1mg/ml in PBS. Protein adsorptions results were shown in Figure 4.19.

Fibrinogen has shown the highest affinity and mass change at all protein concentrations on Trp-SH SAM modified Au surfaces as 2.20 μg/cm^2, 2.00 μg/cm^2, and 5.20 μg/cm^2, respectively. For IgG, delta mass values were measured as follows; 0.60 μg/cm^2, 1.90 μg/cm^2 and 2.22 μg/cm^2 for 0.1 mg/ml, 0.5 mg/ml and 1.0 mg/ml, respectively and were shown in Table 4.10. Albumin has shown no affinity and resulted with negligible interaction between Trp-SH SAM modified surfaces.

Table 4.10
Δ Frequency and Δ mass results of protein adsorption on Trp-SH Modified Au surfaces.

10mM Trp-SH	**Δ Frequency (Hz)**			**Δ Mass (μg/cm^2)**		
Proteins	**0.1mg/ml**	**0.5mg/ml**	**1mg/ml**	**0.1mg/ml**	**0.5mg/ml**	**1mg/ml**
Albumin	None	None	None	None	None	None
Fibrinogen	126.30	111.00	331.40	2.20	2.00	5.20
IgG	31.00	78.00	106.00	0.60	1.90	2.22

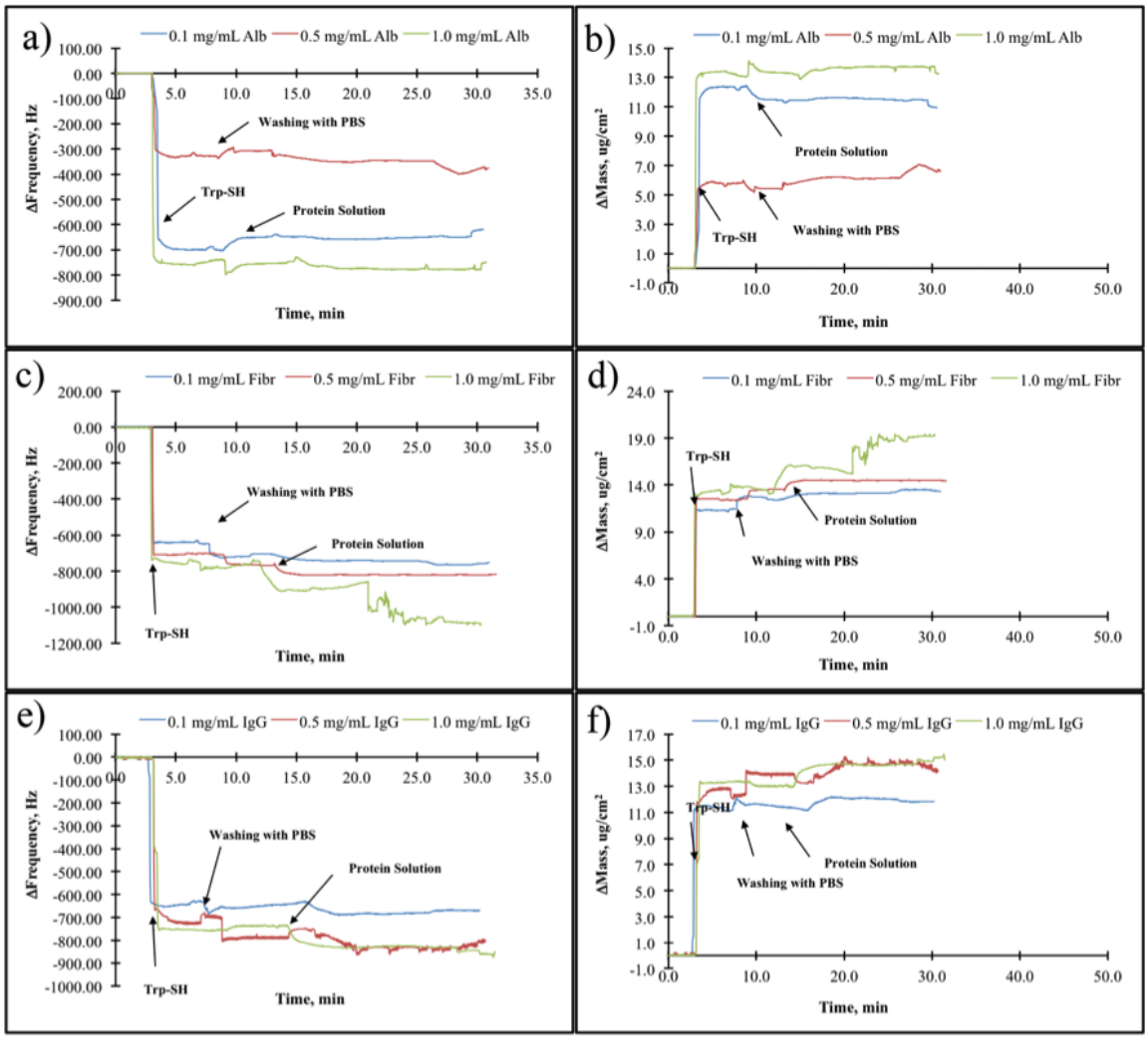

Figure 4.19 Protein adsorption results of 10mM Trp-SH modified Au surface;. a, c, and e are Δ frequency results (Hz); b, d and f are the Δ mass results (μg/cm^2) of protein adsorption in PBS: 7.4 at RT.

5. DISCUSSION

5.1 Surface Modification and Analysis

Surface modifications biomaterials have attracted considerable attention over several decades to increase their biological performances especially their biocompatibility [62]. There are many physicochemical and biological techniques available for the modification biomaterial surfaces to enhance biocompatibility as Thermal spraying [14] [15], Plasma spraying [14] [16], Physical Vapor Deposition (PVD) [14], [17], Chemical Vapor Deposition (CVD) [14] [18], Plasma Enhanced Chemical Vapor Deposition (PECVD) [14], [19] Layer by layer assembly [14], [20], Sol-gel [21] [22], Photolithography [23] Silanization, and Langmuir-Blodgett Deposition [24], Immobilization of biomolecules [16], Spin coating [17], Self-assembled monolayers [16]. Self-assembled monolayers (SAMs) which is the formation of ordered molecular assemblies on selected metallic (Au, Ti, Ag, Cu) and semi-conductor surfaces (Si, GaAs), is an important route to the modification of those surfaces in desired and controllable properties (hydrophilicty, hydrophobicity and functionality such as –SH, –COOH, $–NH_2$, $-CH_3$). These properties are very important because they affect interaction with proteins, cell and biological fluids and tissues [63], [64], [65]. From this point of view, amino acid conjugated SAMs specific to SiO_2 and Au surface were synthesized and their protein adsorption profiles were investigated. SiO_2 and Au surfaces were chosen because of frequently used sensors surfaces for monitoring biocompatibility in terms of protein adsorption [66], [67].

According to our results these amino acid conjugated SAMs are promising molecules because silane heads groups are specific to Titanium (Ti), Silicon (Si), Alumina (Al_2O_3) and Silicone Elastomers such as Polydimethylsiloxane (PDMS) and thiol head groups Au, Ag, Pt and Cu that enables the modification of several different biomaterial surfaces to manipulate protein adsorption behavior using our SAMs [68–74].

5.1.1 ^{1}H-NMR Studies

In this thesis, synthesis of 3 - (trimethoxysilyl) propane amino acids [His-$Si(OCH_3)]_3$ and [Leu-$Si(OCH_3)]_3$ and 3 - mercaptopropanoyl amino acids (3 - mercaptopropanoyl - histidine; 3-mercaptopropanoyl-leucine; 3-mercaptopropanoyl-serine; 3-mercaptopropanoyl- tryptophan) were characterized by ^{1}H-Nuclear Magnetic Resonance Spectroscopy. Amino acid conjugated SAMs for SiO_2 surfaces as [His-$Si(OCH_3)]_3$ and [Leu-$Si(OCH_3)]_3$ were referred to His-Silane SAM, Leu-Silane. Amino acid conjugated SAMs for Au surfaces as 3-mercaptopropanoyl-histidine; 3-mercaptopropanoyl-leucine; 3-mercaptopropanoyl-serine; 3-mercaptopropanoyl-tryptophan were referred to His-SH SAM, Leu-SH SAM, Ser-SH SAM, Trp-SH SAM, respectively.

In the first part of thesis, amino acid conjugated SAMs (His-Silane SAM and Leu-Silane SAM) for SiO_2 surface were synthesized as follow and characterized with ^{1}H-NMR. Cbz group was used as a protective group for amino acids. Amino acids were functionalized from their carboxy functional group using benzotriazole (Bt) as a leaving group. Functionalization of amino acid using benzotriazole helps preservation of chirality of amino acid [75]. For the preparation of His-Silane and Leu-Silane, Cbz protected Histidine (Cbz-His-OH) and Leucine (Cbz-Leu-OH) were converted into N-acylybenzotriazole derivatives Cbz-His-Bt and Cbz-Leu-Bt, respectively. The structure of these compounds was testified from ^{1} H NMR spectrum, where doublet and triplet signals that are belonged to benzotriazole molecule were observed at 8.15-8.30 ppm and 7.50-7.20 ppm, respectively [75]. Also, the aromatic signal with 5 protons that was observed at 7 ppm and the aliphatic signal with 2 protons that was observed at 3.9 ppm, proves the presence of Cbz group. After this step, by the way of nucleophilic substitution of benzotriazole with amine groups, the intermediate products (Cbz-AA-amines) were obtained and these products were determined with the signals at 3.0 ppm, 1.5 ppm and 0.6 ppm which are defined as the three methoxy group signals and the aliphatic -CH_2 signals of amines, respectively. In the end, the protecting groups were separated with catalytic hydrogenation method and the free amine functions were obtained.

In the second part of thesis, amino acids were conjugated with molecules which contains mercapto (-SH) moiety for self-assembling on Au surface. For this purpose, mercapto function of 3-mercaptopropionic acid was protected with acetyl function. After this protection carboxylic acid function of this mercapto acid was functionalized using DCC-BtH methodology to give N-acylbenzotriazole derivative of acetylthiopropanoic acid (3). The characteristic two dublet signals at 8.30-8.00 ppm and two triplet signals between 7.70-7.15 ppm in ^{1} H NMR signals again proves bonding of benzotriazole group [75]. Additionally, the singled signal at 2.45 ppm shows that acetyl group bonded to sulfur. In the second step of reaction, amino acids His-OH, Leu-OH, Ser-OH and Trp-OH were reacted with compound (3) to give substitution with benzotriazole following with deprotection of acetyl group to give 3-mercaptopropanoylamino acids (5). ^{1}H NMR spectrum of compounds 5 have shown no signals corresponding to those assigned to the N-substituted benzotriazole given above. On the other hand characteristic signals for the side groups of amino acids were observed for each amino acids and doublet signal of amid bonding at around the 8.00 ppm to prove bonding of amino acid.

5.1.2 Water Contact Angle Measurements

Water contact angle values of biomaterial surfaces play an important role to investigate and evaluate protein adsorption and cell behavior. As discussed previously by Ratner et al. and Liang et al., surface wettability is very curial and correlated with protein adsorption and cell adhesion [76], [77].

Water contact angle analysis of UV/Ozone treated, 10mM APTES, in situ 10mM amino acid conjugated His-Silane and Leu-Silane modified SiO_2 substrates were investigated. Bare SiO_2 and UV/Ozone treated surfaces contact angle values were measured decreased from $35.8° \pm 2.5 to 8.8 ° \pm 0.6 °$ because of the hydroxylated surface of the SiO_2 surface. The contact angle values were well correlated with the literature [78].

After APTES, His-Silane and Leu-Silane modification water contact angle values

changed significantly to 28.2°±2.0 °, 49.6°±4.9 ° and 68.2°±0.3 °, respectively. APTES modification of SiO_2 surface resulted with increased contact angle value, which could be contributed to modification of APTES molecules on the surface. Slight decrease in hydrophilicity might be due to hydrophobic alkyl groups of APTES molecules. However surface is still hydrophilic because of the amine groups of the APTES molecule and similar results were found where Stefano et al. used APTES molecule to functionalize porous Silicon after oxidizing the surface [78]. Since histidine has a hydrophilic imidazole side chain and (–) 3.2 hydropathy index, His-Silane modified surface has shown a hydrophilic character [79]. When APTES and His-Silane modified surfaces are compared hydrophilicy decreased on His-Silane surfaces. This might be contributed to leaning of His-Silane SAMs due to interaction of imidazole ring of histidine with surface hydroxyl groups of the substrate and alkyl groups of the SAM molecules (originated from APTES molecule) become more accessible and resulted a decrease in hydrophilicity of the surface. On the other hand, the decrease in hydrophilicity is much more evident on Leu-Silane modified surface, due to the aliphatic isobutyl side chain leucine amino acid and alkyl chains of 3-mercaptopropionic acid molecule [21].

Water contact angle analysis of UV/Ozone treated and in situ 10mM amino acid conjugated SH-SAM modified Au substrates were also investigated. Water contact angle value of UV/Ozone treated surface was measured to be 26.5°±6.7 ° due to oxide formation on the Au surface [58], [80]. Au substrates were then immersed in absolute ethanol for 1 hour and water contact angle values were found to be 61.9°±9.3 ° as an evidence of the reduction of oxides [58], [80]. Amino acid conjugated –SH SAMs (histidine, leucine, serine, and tryptohan) have shown no significant difference in water contact angle values after modification as 65.3°±2.7 °, 63.9°±4.3 °, 70.4°±1.4 °, 69.0°±1.3 °, respectively. This may be concluded to similar surface coverage, interaction of side chains of amino acids with Au surface and leaning of -SH SAMs that introduce hydrophobic alkyl chains of 3-mercaptopropionic acid molecule [81], [82].

5.1.3 Optimization of SAM Immobilization on SiO_2 and Au QCM Crystals

His-SH used as a reference SAM to determine the optimum concentration of amino acid conjugated SAMs for in-situ surface modification of QCM crystals. 10-80mM (in absolute ethanol) His-SH solutions were used to modify Au QCM surfaces. The amount (in terms of mass) of immobilized SAMs was changed between 8.00-13.00 $\mu g/cm^2$. According to the measurements highest His-SH SAM immobilization was measured when 10mM SAM was used and found to be 13.00 $\mu g/cm^2$. From these results optimum concentration of solution was determined as 10mM and it was clearly observed that concentration has no effect on Δ frequency (Hz) and Δ mass change on Au surfaces. This situation could be explained by the saturation of Au surface by the interaction of sulfur with Au atoms [83]. Another explanation could be because of the steric hindrance of side chain of Histidine that inhibits the interaction and accessibility of free SAMs in the solution to the surface [81], [82]. This situation might contribute to all other type of amino acid conjugated SAMs that were used in this thesis.

5.2 Protein Adsorption Studies

It is well known that properties proteins and surfaces affect their interactions visa versa. For protein properties such as size, charge, structure stability and folding rate for surface properties such as topography, composition, hydrophobicity, heterogeneity and potential affect their interactions with proteins and surfaces [63]. When we investigated the non-specific protein adsorption of amino acid conjugated SAM modified SiO_2 and Au substrates by QCM sensor, for SiO_2 surfaces; fibrinogen has shown the highest affinity and mass change while IgG has shown the lowest affinity and mass values at 0.5mg/ml protein concentration. This situation may be explained by the point of view of the size of the proteins. Fibrinogen IgG and Albumin molecular weights are 340 kDa, 153 kDa and 66.7 kDa, respectively [84], [85].

As fibrinogen has the largest protein of all, it may show the highest affinity to the surface due to having more sites of contact with the surface. It is also well known

that proteins tend to adsorb more at their isoelectric point (IP) [87] IgG was expected to adsorb more (all experiments were in PBS). IP of Fibrinogen, IgG and Albumin are 5.5, 6.4-7.6, 4.7, respectively [86] [87], [88]. However, IgG adsorption was the lowest for SiO_2 surfaces. From these results we may concluded that (1) size of a protein is much more predominant for fibrinogen, (2) surface hydrophilicity is predominate then IP for IgG (3) other factors (composition, potential) might be considered for the adsorption of Albumin. For Au surface, like SiO_2 surface; fibrinogen has shown the highest affinity and mass change while IgG has shown the lowest affinity and mass values at 0.5mg/ml protein concentration. From these results we may concluded that (1) increased hydrophobicity and due to the size of the fibrinogen, more fibrinogen adsorbed to Au surface (2) other factors such as composition, potential might be predominate since surface hydrophobicity increased and pH is very close to IP of IgG, but IgG has shown the lowest affinity, (3) hydrophobicity is more dominant then IP for Albumin, since its adsorption was increased. Including to that since Au surface is more hydrophobic then SiO_2 surface it is reasonable that all proteins have shown higher adsorption amounts [63], [88], [89].

The effect of protein concentration on non-specific adsorption was investigated and three different concentrations of target protein adsorption (albumin, fibrinogen and IgG) were carried out on bare Au surfaces. Similar amounts of Albumin and Fibrinogen adsorbed at 0.1 and 0.5 mg/ml concentrations to Au surface and the decreased when at 1.0 mg/ml concentration. We may conclude that surface coverage was achieved at 0.5mg/ml concentration. Also, lateral interaction between Albumin and Fibrinogen proteins may be increased thus resulted with the less protein adsorption at 1.0 mg/ml concentration [90].

To evaluate the effect of surface chemistry and wettability to protein adsorption SiO_2 surfaces were modified with 10mM APTES, His-Silane and Leu-Silane SAMs. The concentrations of target proteins (albumin, fibrinogen and IgG) were prepared between 0.1-1mg/ml in PBS.

The protein affinity to His-Silane modified surfaces was found to be in that order

Fibrinogen > Albumin > IgG. For all proteins, increasing the protein concentration resulted with increased mass change. This result may be concluded to the high affinity of Fibrinogen to histidine amino acid. Since histidine is hydrophilic with a -3.2 hydropathy index, the affinity of Fibrinogen might come from its chemical structure, the imidazole ring [91].

The lower affinity of Albumin and IgG were a result of hydrophilic surface, which might be hydrophilicity, more dominant then surface chemistry for these proteins a resulted decrease protein adsorption [63]. For relatively more hydrophobic surface as Leu-Silane SAM modified SiO_2 surfaces, IgG has shown the highest affinity a 0.1 mg/ml concentration, for 0.5 and 1.0 mg/ml concentrations, Fibrinogen has shown the highest adsorption capacity. For 0.1 mg/ml, protein affinity to Leu-Silane modified surfaces was found to be in that order IgG > Fibrinogen > Albumin. 0.5 and 1.0 mg/ml concentrations was found to be in that order, Fibrinogen > Albumin > IgG. For lower concentration, lateral interaction of Albumin and Fibrinogen might be higher that their adsorption capacity decreased [90]. For a general comment may be done that Fibrinogen has shown higher affinity due to the hydrophobic structure of Leu-Silane then Albumin and IgG. APTES was used to the effect of conventional SAM molecule on protein adsorption. The protein affinity to APTES modified surfaces was found to be for 0.1 and 0.5 mg/ml concentrations in that order Fibrinogen>Albumin>IgG and for 1.0 mg/ml concentration Albumin>IgG >Fibrinogen that is totally different behavior then amino acid conjugated SAMs. An overall commend can be done as follows,

1. Fibrinogen has shown the highest affinity to His-Silane SAM. Surface chemistry (imidazole ring of histidine) is more dominant then surface hydrophilicity for Fibrinogen. Fibrinogen has shown the lowest affinity to APTES, which is more hydrophilic then Histidine [90].

2. Albumin and IgG have higher affinity to Leu-Silane and APTES SAM then His-Silane. Hydrophobicity and chemical structure are dominant factors for Albumin and IgG. More studies should be performed [63]. To evaluate the effect of surface chemistry and wettability to protein adsorption Au surfaces were modified with

10mM His-SH, Leu-SH, Ser-SH and Trp-SH. The concentrations of target proteins (albumin, fibrinogen and IgG) were prepared between 0.1-1mg/ml in PBS.

3. No affinity was observed on His-SH modified Au surfaces to Albumin. Fibrinogen and IgG have shown low affinity and mass change to His-SH modified Au surfaces. Basically protein repellent surface was obtained by using His-SH modification on Au surfaces. Water contact angle measurements showed that surface has a angle of 65.3°±2.7 °, a semi hydrophilic surface expected to show an adsorption behavior. This may contributed to interaction of side chain of Histidine amino acid with Au surface and each other were much more higher then the interaction with proteins. More studies should be done to identify the type of interactions. For Leu-SH SAM modified Au surfaces, IgG has shown the highest affinity a 0.1 mg/ml concentration, for 0.5 and 1.0 mg/ml concentrations, Fibrinogen has shown the highest adsorption capacity. For 0.1 mg/ml, protein affinity to Leu-Silane modified surfaces was found to be in that order IgG > Fibrinogen > Albumin. 0.5 and 1.0 mg/ml concentrations was found to be in that order, Fibrinogen > Albumin > IgG. For lower concentration, lateral interaction of albumin and fibrinogen might be higher that their adsorption capacity decreased [90]. For a general comment may be done that Fibrinogen has shown higher affinity due to the chemical structure of Leu-SH then Albumin and IgG [91].

4. Protein adsorption to Ser-SH and Trp-SH SAM modified surfaces have shown similar behavior as His-SH, which is less interaction with all type of proteins that are used in this study. Serine and Tryptophan amino acids hydropathy indexes are -0.8 and -0.9, respectively [79].

Their values are very close to each other and their protein repellent response might be the result of having moderate hydrophilicity of the surface after modification. An overall commend can be done as follows,

1. Fibrinogen has shown the highest affinity to Leu-SH SAM. Surface chemistry (alkyl groups of leucine amino acid side chain) is more dominant then surface

hydrophilicity [91]. Leu-SH modified Au surfaces have shown higher affinity to all proteins.

2. Fibrinogen has shown the highest affinity to Leu-SH SAM. Surface chemistry (alkyl groups of leucine amino acid side chain) is more dominant then surface hydrophilicity [91].

3. Since the hydrophilicty of SH-SAM modified surfaces are same, interaction of side chains to each other and/or the interaction of the sides chains with Au surface should be more strong then the interactions with proteins for His-SH, Ser-SH and Trp-SH SAMs [89].

4. Surface coverage is an important parameter that should be explained in order to understand the interaction of SAMs, proteins, and surfaces to each other.

5. When we compare, His-Silane and His-SH, properties of surfaces have shown a clear difference and effect on protein adsorption.

6. When we compare, Leu-Silane and Leu-SH, properties of surfaces have shown a clear effect on protein adsorption as having the same surface chemistry.

Over all, surface type, surface chemistry, surface wettability and surface orientation of molecules have an effect on the protein adsorption. Depending to the purpose protein attractive and repellent surfaces can be prepared and might find several different application in biomaterial science

5.3 Future Studies

Protein adsorption studies will give important clue for the investigation of biocompatibility, but more studies should be performed to evaluate biocompatibility totally. For this purpose cell studies should be done and cellular behavior such as proliferation, adhesion, differentiation with model cells (Fibroblast and PC12) will be studied. Including to those studies, glycoaminoglycans, which are constituents of the extracellular matrix as amino acid conjugated self-assembled monolayers, will be synthesized in form of self-assembled monolayers. Their protein interactions and effects on cell behavior will be examined in our future research in this field.

REFERENCES

1. Langer, R., and D. A. Tirell, "Designing materials for biology and medicine," *Nature*, Vol. 428, pp. 482–497, April 2004.

2. N Stephanopoulos, J H, O., and S. I. Stupp, "Self-assembly for the synthesis of functional biomaterials," *Acta Materialia*, Vol. 61, pp. 912–930, 2013.

3. Weiss, P. S., "Functional molecules and assemblies in controlled environments: Formation and measurements," *Acc. Chem. Res.*, Vol. 41, pp. 1772–1781, 2008.

4. Khatayevich, D., M. Gungormus, , C. So, S. Cetinel, , H. Ma, A. Jen, C. Tamerler, and M. Sarikaya, "Biofunctionalization of materials for implants using engineered peptides," *Acta Biomaterialia*, Vol. 6, pp. 4634–4641, 2010.

5. Thourson, S. B., C. A. Marsh, B. J. Doyle, and S. J. Timpe, "Quartz crystal microbalance study of bovine serum albumin adsorption onto self-assembled monolayer-functionalized gold with subsequent ligand binding," *Colloids and Surfaces B: Biointerfaces*, Vol. 111, pp. 707–712, 2013.

6. Yang, D., X. Lu, Y. Hong, T. Xi, and D. Zhang, "The molecular mechanism of mediation of adsorbed serum proteins to endothelial cells adhesion and growth on biomaterials," *Biomaterials*, Vol. 34, pp. 5747–5758, 2013.

7. Feiler, A. A., A. Sahlholm, T. Sandberg, and K. D. Caldwell, "Adsorption and viscoelastic properties of fractionated mucin (bsm) and bovine serum albumin (bsa) studied with quartz crystal microbalance (qcm-d)," *Journal of Colloid and Interface Science*, Vol. 315, pp. 475–481, 2007.

8. Jr, R. M. P., and K. Uvdal, "Arg–cys and arg–cysteamine adsorbed on gold and the g-protein–adsorbate interaction," *Colloids and Surfaces B: Biointerfaces*, Vol. 25, pp. 335–346, 2002.

9. Ogi, H., K. Motohisa, K. Hatanaka, T. Ohmori, M. Hirao, and M. Nishiyama, "Concentration dependence of igg–protein a affinity studied by wireless-electrodeless qcm," *Biosensors and Bioelectronics*, Vol. 22, pp. 3238–3242, 2007.

10. Bhure, R., A. Mahapatro, C. Bonner, and T. M. Abdel-Fattah, "In vitro stability study of organophosphonic self assembled monolayers (sams) on cobalt chromium (co–cr) alloy," *Materials Science and Engineering C*, Vol. 33, p. 2050–2058, 2013.

11. Huebsch, N., and D. J. Mooney, "Inspiration and application in the evolution of biomaterials," *Nature*, Vol. 462, pp. 426–432, November 2009.

12. Xu, L., J. W. Bauer, and C. A. Siedlecki, "Proteins, platelets, and blood coagulation at biomaterial interfaces," *Colloids and Surfaces B: Biointerfaces*, Vol. 124, pp. 49—-68, 2014.

13. Chu, P. K., "Surface engineering and modification of biomaterials," *Thin Solid Films*, Vol. 528, pp. 93–105, January 2013.

14. Agrawal C M, Ong J L, A. M. R. M. G., *Introduction to Biomaterials: Basic Theory with Engineering Applications*, Cambridge University Press, first ed., 2013.

15. Bolelli, G., D. Bellucci, V. Cannillo, L. Lusvarghi, A. Sola, N. Stiegler, P. Müller, A. Killinger, R. Gadow, L. Altomare, and L. D. Nardo, "Suspension thermal spraying of hydroxyapatite: Microstructure and in vitro behavior," *Materials Science and Engineering:C*, Vol. 34, pp. 287–303, January 2014.

16. Heimann, R., *Plasma-Spray Coating: Principles and Applications*, John Wiley & Son, first ed., 2008.

17. Reyes-Figueroa, P., T. Painchaud, T. Lepetit, S. Harel, L. Arzel, J. Yi, N. Barreau, and S. Velumani, "Structural properties of in_2se_3 precursor layers deposited by spray pyrolysis and physical vapor deposition for $cuinse_2$ thin-film solar cell applications," *Thin Solid Films*, Vol. 587, pp. 112–116, July 2015.

18. Park, S. W., D. Lee, H. R. Lee, H. J. Moon, B. R. Lee, W. Ko, S. J. Song, S. J. Lee, K. Shin, W. Jang, J. Yi, S. G. Im, and I. K. Kwon, "Generation of functionalized polymer nanolayer on implant surface via initiated chemical vapor deposition (icvd)," *Journal of Colloid and Interface Science*, Vol. 439, pp. 34–41, February 2015.

19. Chhowalla, M., K. Teo, C. Ducati, N. Rupensinghe, G. A. J. Amaratunga, A. C. Ferrari, D. Roy, J. Robertson, and W. I. Milne, "Growth process conditions of vertically aligned carbon nanotubes using plasma enhanced chemical vapor deposition," *Journal of Applied Physichs*, Vol. 90, pp. 5038–5317, 2001.

20. Aslan, S., M. Deneufchatel, S. Hashmi, N. Li, L. D. Pfefferle, M. Elimelech, E. Pauthe, and P. R. V. Tassel, "Carbon nanotube-based antimicrobial biomaterials formed via layer-by-layer assembly with polypeptides," *Journal of Colloid and Interface Science*, Vol. 388, pp. 269–273, December 201.

21. Mahapatro, A., "Bio-functional nano-coatings on metallic biomaterials," *Materials Science and Engineering: C*, Vol. 55, pp. 227–251, October 2015.

22. Poongodi, G., P. Anandan, R. M. Kumar, and R. Jayavel, "Studies on visible light photocatalytic and antibacterial activities of nanostructured cobalt doped zno thin films prepared by sol-gel spin coating method," *Spectrochimica Acta Part A: Molecular and Biomolecular Spectroscopy*, Vol. 148, pp. 237–240, September 2015.

23. Rena, H. X., X. J. Huang, J. H. Kim, Y. K. Choi, and N. Gu, "Pt/au bimetallic hierarchical structure with micro/nano-array via photolithography and electrochemical synthesis: From design to got and gpt biosensors," *Talanta*, Vol. 78, pp. 1371–1377, June 2009.

24. Schreiber, F., "Structure and growth of self-assembling monolayers," *Progress in Surface Science*, Vol. 65, pp. 151–257, November-December 2000.

25. Dubrovsky, T., A. Tronin, S. Dubrovskaya, S. Vakula, and C. Nicolini, "Immunological activity of igg langmuir films oriented by protein a sublayer," *Langmuir films*, Vol. 23, pp. 1–7, 1995.

26. Vadgama, P., *Surfaces and Interfaces for Biomaterials*, Woodhead Publishing, first ed., 2005.

27. Hernandez-Montelongo, J., D. Gallach, N. Naveas, V. Torres-Costa, A. Climent-Font, J. García-Ruiz, and M. Manso-Silvan, "Calcium phosphate/porous silicon biocomposites prepared by cyclic deposition methods: Spin coating vs electrochemical activation," *Materials Science and Engineering: C*, Vol. 34, pp. 245–251, January 2014.

28. Luna, D. M., K. Y. Avelino, M. T. Cordeiro, C. A. Andrade, and M. D. L. Oliveira, "Electrochemical immunosensor for dengue virus serotypes based on 4-mercaptobenzoic acid modified gold nanoparticles on self-assembled cysteine monolayers," *Sensors and Actuators B: Chemical*, Vol. 220, pp. 565–572, December 2015.

29. Shervedani, R. K., M. S. Foroushani, and S. B. Dehaghi, "Functionalization of gold mercaptopropionic acid self-assembled monolayer with 5-amino-1,10-phenanthroline: Interaction with iron(ii) and application for selective recognition of guanine," *Electrochimica Acta*, Vol. 164, pp. 344– 352, May 2015.

30. Spencer, N. D., *Tailoring Surfaces: Modifying Surface Composition and Structure for Applications in Tribology, Biology and Catalysis*, World Scientific, first ed., 2011.

31. SRS, S., "Qcm 200 quartz crystal microbalance digital controller manual." www.thinksrs.com/downloads/PDFs/Manuals/QCM200m.pdf, 2011.

32. Xu, W., K. Bai, J. He, W. Su, L. Dong, L. Zhang, and T. Wang, "Leucine improves growth performance of intrauterine growth retardation piglets by modifying gene and protein expression related to protein synthesis," *Nutrition*, July 2015.

33. Aguilar, M., and I. Aguilar, *HPLC of Peptides and Proteins Methods and Protocols*, Humana Press, first ed., 2004.

34. Haney, E. F., A. P. Petersen, C. K. Lau, W. Jing, D. G. Storey, and H. J. Vogel, "Mechanism of action of puroindoline derived tryptophan-rich antimicrobial peptides," *Biochimica et Biophysica Acta (BBA) – Biomembranes*, Vol. 1828, pp. 1082–1813, August 2013.

35. Koolman, J., and K. H. Roehm, *Color Atlas of Biochemistry*, Humana Press, second ed., 2005.

36. Aparicio, C., F. J. Gil, U. Thams, F. Munoz, A. Padroz, and J. Planell, "Osseointegration of gritblasted and bioactive titanium implants: Histomorphometry in minipigs," *Key engineering materials*, Vol. 254, pp. 737–740, 2004.

37. Lange, R., U. Beck, J. Rychly, A. Baunman, and B. Nebe, "Cell-extracellular matrix interaction and physic-chemical characteristics of titanium surfaces depend on the roughness of the material," *Biomolecular Engineering*, Vol. 19, pp. 255–261, 2002.

38. Acton, Q. A., *Advances in Immunoglobulin G Research and Application*, HScholarlyBrief, first ed., 2011.

39. Hemersam, A. G., M. Foss, J. Chevallier, and F. Besenbacher, "Adsorption of fibrinogen on tantalum oxide, titanium oxide and gold studied by the qcm-d technique," *Colloids and Surfaces B- Biointerfaces*, Vol. 43, pp. 208–215, 2005.

40. Yongli, C., Z. Xiufang, G. Yandao, Z. Namning, Z. Tingying, and S. Xinqi, "Conformational changes of fibrinogen adsorption onto hydroxyapatite and titanium oxide nanoparticles," *Journal of Colloid and Interface Science*, Vol. 214, pp. 38–45, 1999.

41. Pandey, L. M., and S. Pattanayek, "Properties of competitively adsorbed bsa and fibrinogen from their mixture on mixed and hybrid surfaces," *Applied Surface Science*, Vol. 264, pp. 832–837, January 2013.

42. Bhakta, S. A., E. Evans, T. E. Benavidez, and C. D. Garcia, "Protein adsorption onto nanomaterials for the development of biosensors and analytical devices: A review," *Analytica Chimica Acta*, Vol. 872, pp. 7–25, May 2015.

43. Puleo, D. A., and R. Bizios, *Biological Interactions on Materials Surfaces: Understanding and Controlling Protein, Cell and Tissue Responses*, Springer, first ed., 2009.

44. Norde, W., and J. Lyklema, "Why proteins prefer interfaces," *Journal of Biomaterials Science Polymer*, Vol. 2, pp. 183–202, - 1991.

45. Tengvall, P., , D. Brunette, M. Textor, and P. Thomsen, "Proteins at titanium interfaces," *in Titanium in Medicine*, Vol. Springer, pp. 458–480, - 2001.

46. F, H., "Development of novel qcm technique for protein adsorption studies," Master's thesis, Chalmers University of Technology and Göteborg University, 1997.

47. Zhang, S., L. Li, and A. Kumar, *Materials Characterization Techniques*, Crc Press,, first ed., 2008.

48. Ogi, H., K. Motohisa, K. Hatanaka, T. Ohmori, M. Hirao, and M. Nishiyama, "Concentration dependence of igg–protein a affinity studied by wireless-electrodeless qcm," *Biosensors and Bioelectronics*, Vol. 22, p. 3238–3242, June 2007.

49. D. S. Ballantine, R. M. White, S. J. M. A. J. R. E. T. Z. G. C. F., and H. Woltjen, *Acoustic Wave Sensors: Theory, Design and Physico-Chemical Applications*, Acad Press, first ed., 1997.

50. Guilbault, G. G., and J. Jordan, "Analytical uses of piezoelectric crystals," *CRC Reviews*, Vol. 19, pp. 1–28, 1964.

51. King, W. H., "Piezoelectric sorption detector," *Anal. Chem.*, Vol. 36, p. 1735, 1964.

52. Ben-dov, and I. Willmer, "Piezoelectric immunosensors for urine specimens chlamidia trachomatis employing qcm microgravimetric analysis," *Anal. Chem.*, Vol. 69, p. 3506, 1997.

53. Storri, S., "Surface modifications for the development of piezoimmunosensors," *Biosensors and Bioelectronics*, Vol. 13, p. 347, 1998.

54. Tajima, I., "Monitor of antibodies in human saliva using a piezoelectric qc biosensor," *Anal. Chim. Acta*, Vol. 365, pp. 147–149, 1998.

55. Liu, Y.-C., C.-M. Wang, and K.-P. Hsiung, "Comparison of different protein immobilization methods on quartz crystal microbalance surface in flow injection immunoassay," *Analytical Biochemistry*, Vol. 299, pp. 130– 135, 2001.

56. Katritzky, A. R., P. Angrish, D. Hür, and K. Suzuki, "N-(cbz- and fmoc–aminoacyl)benzotriazoles: Stable derivatives enabling peptide coupling of tyr, trp, cys, met, and gln with free amino acids in aqueous media with complete retention of chirality," *Synthesis*, Vol. 3, p. 397–402, 2005.

57. Systems, S. R., "Qcm200 quartz crystal microbalance digital controller manual." www.thinksrs.com/downloads/PDFs/Manuals/QCM200m.pdf, 2011.

58. Woodward, J. T., M. L. Walker, C. W. Meuse, D. J. Vanderah, G. E. Poirier, and A. L. Plant, "Effect of an oxidized gold substrate on alkanethiol self-assembly," *Langmuir*, Vol. 16, pp. 347– 5353, 2000.

59. Kankare, J., "Sauerbrey equation of quartz crystal microbalance in liquid medium," *Langmuir*, Vol. 18, pp. 7092–7094, 2002.

60. Han, Y., D. Mayer, A. O. enhausser, , and S. Ingebrandt, "Surface activation of thin silicon oxides by wet cleaning and silanization," *Thin Solid Films*, Vol. 510, pp. 175–180, 2006.

61. B. Colbert, J. Ankney, J. W. J. H., *An Integrated Approach to Health Sciences: Anatomy and Physiology, Math, Chemistry and Medical Microbiology*, Delmar Congage Learning, second ed., 2011.

62. Tverdokhlebov, S., E. Bolbasov, E. Shesterikov, L. Antonova, A. Golovkin, V. Matveeva, D. Petlin, and Y. Anissimov, "Modification of polylactic acid surface using rf plasma discharge with sputter deposition of a hydroxyapatite target for increased biocompatibility," *Applied Surface Science*, Vol. 329, pp. 32–39, February 2015.

63. C., D. K., and P. D. A., "Protein-surface interactions," *in An Introduction to Tissue-Biomaterial Interactions*, pp. 37–52: Wiley, 2002.

64. Raffaini, G., and F. Ganazzoli, "Surface topography effects in protein adsorption on nanostructured carbon allotropes," *Langmuir*, Vol. 29, p. 4883–4893, 2013.

65. Botelho, C. M., R. Brooks, M. Kanitakahara, C. Ohtsuki, S. Best, M. A. Lopers, N. Rushton, W. Bonfield, and J. D. Santos, "Effect of protein adsorption onto the dissolution of silicon-substituted hydroxyapatite," *Journal of Encapsulation and Adsorption Sciences*, Vol. 1, pp. pp 72–79, 2011.

66. Chen, H., X. Su, K. G. Neoh, and W. Choe, "Qcm-d analysis of binding mechanism of phage particles displaying a constrained heptapeptide with specific affinity to si02 and tio2," *Anal. Chem.*, Vol. 72, pp. pp 4872– 4879, 2006.

67. Stadler, H., M. Mondon, and C. Ziegler, "Protein adsorption on surfaces: dynamic contact-angle (dca) and quartz-crystal microbalance (qcm) measurements," *Anal. Bioanal. Chem*, Vol. 375, p. 53–61, 2003.

68. Egger, D. A., F. Rissner, G. M. Rangger, O. T. Hofmann, L. Wittwer, G. Heimel, and E. Zojer, "Self-assembled monolayers of polar molecules on au(111) surfaces: distributing the dipoles," *Physical Chemistry Chemical Physics*, Vol. 12, pp. 4291–4294, 2010.

69. Baviloliaei, M. S., and L. Diekhöner, "Molecular self-assembly at nanometer scale modulated surfaces: trimesic acid on ag(111), cu(111) and ag/cu(111)," *Physical Chemistry Chemical Physics*, Vol. 16, pp. 11265–11269, 2014.

70. Lee, S., J. Park, R. Ragan, S. Kim, Z. Lee, D. K. Lim, D. A. A. Ohlberg, and R. S. Williams, "Self-assembled monolayers on pt(111): Molecular packing structure and strain effects observed by scanning tunneling microscopy," *J. AM. CHEM. SOC.*, Vol. 128, pp. 5745–5750, 2006.

71. Godlewski, S., and M. Szymonski, "Adsorption and self-assembly of large polycyclic molecules on the surfaces of tio2 single crystals," *International Journal of Molecular Sciences*, Vol. 14, pp. 2946–2966, 2013.

72. Wang, Y., M. Lieberman, Q. Hang, and G. Bernstein, "Selective binding, self-assembly and nanopatterning of the creutz-taube ion on surfaces," *International Journal of Molecular Sciences*, Vol. 10, pp. 533–558, 2009.

73. DiBenedetto, S. A., A. Facchetti, M. A. Ratner, , and T. J. Marks, "Molecular self-assembled monolayers and multilayers for organic and unconventional inorganic thin-film transistor applications," *Advanced Materials*, Vol. 21, pp. 1407–1433, 2009.

74. Kuddannaya, S., Y. J. Chuah, M. H. A. Lee, N. V. Menon, Y. Kang, and Y. Zhang, "Surface chemical modification of poly(dimethylsiloxane) for the enhanced adhesion and proliferation of mesenchymal stem cells," *Applied Materials Interfaces*, Vol. 5, p. 97779784, 2013.

75. Hür, D., S. F. Ekti, and R. Say, "N-acylbenzotriazole mediated synthesis of some methacrylamido amino acids," *Letters in Organic Chemistry*, Vol. 4, pp. 585–587, 2007.

76. Hao, L., and J. Lawrence, *Laser Surface Treatment of Bio-Implant Materials*, John Wiley Sons Ltd, 2005.

77. Ratner, B. D., A. S. H. F. J. S., and J. E. Lemons, *Biomaterials science An Introduction to Materials in Medicine.*, California: Academic Press, 1996.

78. Stefano, L. D., G. Oliviero, J. Amato, N. Borbone, G. Piccialli, L. Mayol, I. R. M. Terracciano, and I. Rea, "Aminosilane functionalizations of mesoporous oxidized silicon for oligonucleotide synthesis and detection," *J R Soc Interface*, Vol. 10, pp. 1–7, 2013.

79. E.Foulquier, and C.Ginestoux, "Hydropathy index." imgt.org/IMGTeducation/Aide-memoire/_UK/aminoacids, 2013.

80. D, L., "In-situ characterization of self-assembled monolayers of water-soluble oligo (ethylene oxide) compounds," *Colloids and Surfaces B: Biointerfaces*, Vol. 82, pp. 450–455, 2011.

81. B, A., "Amino acid conjugated self assembly molecules modified si wafers"," Master's thesis, Boğaziçi University, Istanbul, Turkey, 2014.

82. Öztürk M. Ö, "Preparation and characterization of cartilage mimicked structures," Master's thesis, Boğaziçi University, Istanbul, Turkey, 2014.

83. Häkkinen, H., "The gold–sulfur interface at the nanoscale," *Nature Chemistry*, Vol. 4, p. 443–455, 2012.

84. Quinlan, G. J., G. S. Martin, and T. W. Evans, "Albumin: Biochemical properties and therapeutic potential," *Hepatology*, Vol. 41, pp. 1211–1219, June 2005.

85. M., D. T., *Textbook of Biochemisty*, Wiley, seventh ed., 2010.

86. Danielsson, , A. Ljunglöf, and H. Lindblom, "One-step purification of monoclonal igg antibodies from mouse ascites : An evaluation of different adsorption techniques using high performance liquid chromatography," Vol. 15, pp. 79–88, 1988.

87. Vlasova, I. M., and A. M. Saletsky, "Study of the denaturation of human serum albumin by sodium dodecyl sulfate using the intrinsic fluorescence of albumin," *Journal of Applied Spectroscopy*, Vol. 76, pp. 536–541, 2006.

88. Salim, M., B. O'Sullivan, S. L. McArthur, and P. C. Wright, "Characterization of fibrinogen adsorption onto glass microcapillary surfaces by elisa," *Lab Chip*, Vol. 7, pp. 64–70, 2007.

89. Brown, N. L., S. P. Bottomley, M. D. Scawen, and M. G. Gore, "A study of the interactions between an igg-binding domain based on the b domain of staphylococcal protein a and rabbit igg," *Molecular biotechnology*, Vol. 10, pp. 9–16, 1998.

90. Kurylowicz, M., H. Paulin, J. Mogyoros, M. Giuliani, and J. R. Dutcher, "The effect of nanoscale surface curvature on the oligomerization of surface-bound proteins," *J. R. Interface*, Vol. 11, pp. 1–9, 2013.

91. Jones, A. L., M. D. Hulett, and C. R. Parish, "Histidine-rich glycoprotein: A novel adaptor protein in plasma that modulates the immune, vascular and coagulation systems," *Immunology and Cell Biology*, Vol. 83, pp. 106–118, 2005.